

1 **Mediterranean Badlands: their driving processes and climate change futures**

2 Nadal-Romero, E.¹, Rodríguez-Caballero, E.^{2,3}, Chamizo, S.^{2,3}, Juez, C.¹, Cantón, Y.,^{2,3}
3 García-Ruiz, J.M.¹

4 ¹ Instituto Pirenaico de Ecología, Consejo Superior de Investigaciones Científicas (IPE-
5 CSIC), Campus de Aula Dei, P.O. Box 13.034, Zaragoza, Spain

6 ² Department of Agronomy (Soil Science Area), University of Almería, Engineering High
7 School, Almería, Spain

8 ³ Centro de Investigación de Colecciones Científicas de la Universidad de Almería
9 (CECOUAL), University of Almería, 04120 Almería, Spain

10

11 **Abstract**

12 Badlands are landforms that occur all over the World. In the Mediterranean region,
13 badlands are found in both dry (arid and semiarid) and wet (subhumid and humid)
14 environments, and are characterized by complex hydro-geomorphological
15 dynamics, high intense erosion processes and extreme sediment yield.
16 Understanding the impact of Global Change is key to predict the on-site and off-site
17 effects on badland dynamics, particularly its consequences on bedrock weathering,
18 on sediment yield and delivery and on plant colonization. Here, conducting a
19 systematic literature review, we analyzed an extensive database and identified the
20 main climate-drivers affecting the hydro-geomorphological dynamics in
21 Mediterranean badlands (based on Non-Metric MultiDimensional Scaling and
22 Structural Equation Modelling analysis). Later, we examined the main impacts
23 expected from climate change forecasting in the near future, and we explored the
24 interactions between badlands response to climate variation. In Mediterranean
25 badlands, weathering processes are mainly related to wetting-drying cycles and
26 freeze-thaw cycles in dry and wet badlands, respectively. In both environments,

27 rainfall amount appears as the main driver for runoff response, and rainfall amount
28 and rainfall intensity for erosion dynamics. Future climate scenarios forecast a
29 decrease in annual rainfall, number of rainfall events and frost days, and in soil
30 moisture, and an increase in rainfall intensity. These changes will have direct hydro-
31 geomorphological implications with direct and indirect effects on badland dynamics.
32 This may result in a decrease in annual runoff in dry badlands, but the occurrence
33 of more frequent extreme events would increase soil erosion and could negatively
34 affect biological soil crust. In wet badlands, weathering and erosion processes may
35 decrease, and a stabilization of the slopes, with consequently improved vegetation
36 growth, may be expected. In addition, the forecasted changes must be taken into
37 account, especially considering the possible off-site effects of these extreme
38 environments.

39

40 **Keywords:** badlands, Global Change, climate change, weathering, erosion,
41 hydrology

42

43 **1. Introduction**

44 Badlands have been defined by different criteria in the last decades (i.e. Bryan and
45 Yair, 1982; Fairbridge, 1968; Gallart *et al.*, 2002; Torri *et al.*, 2013). Most definitions
46 agreed that badlands are landforms developed on soft or poorly consolidated
47 bedrock with limited plant cover, where a wide range of geomorphic processes play
48 a paramount role, including weathering and erosion (Martínez-Murillo and Nadal-
49 Romero, 2018). Badlands develop in a large variety of climatic regions and on a
50 relatively wide range of lithologies. Nevertheless, the geomorphic processes

51 contributing to badland evolution show a large spatial and temporal variability, in
52 spite of which badlands tend to produce converging geoforms (Kasanin-Grubin and
53 Bryan, 2007). The particular topographic and lithologic conditions, as well as the
54 rapid changes these systems undergo in short periods of time and the changes
55 observed in the surrounding areas (i.e. abandonment of grazing activities), result in
56 badlands with a huge interest from a geomorphological, ecological, educational,
57 economic and social point of view. All these attributes make badlands excellent
58 research laboratories for the study of hydro-geomorphological processes at an
59 affordable human scale, and particularly make these systems especially interesting
60 to study processes involved in Global Change (Nadal-Romero and García-Ruiz,
61 2018).

62 From a geomorphological point of view, the hydrological and erosion responses are
63 extremes, especially in subhumid and humid badlands, showing important on-site
64 and off-site implications. The occurrence of high erosion rates modifies the physical
65 properties of the regolith, causes a loss of nutrients and destabilizes the hillslopes
66 hindering plant colonization (Cantón *et al.*, 2018). Moreover, water and sediment
67 fluxes, originated in badland areas during rainstorms, very often provoke severe
68 environmental and economic off-site effects, such as channel silting, sediment
69 accumulation in the alluvial plain, reservoir sedimentation (Copard *et al.*, 2018),
70 reducing the quality of water for domestic and industrial uses, which in turn may
71 produce important economic impacts (Pimentel *et al.*, 1995).

72 From an ecological perspective, the extreme environmental conditions of badlands,
73 (e.g. the high slope gradients and instability) configure a high variety of microclimatic
74 conditions (Rodríguez-Caballero *et al.*, 2019), which contribute to a high biodiversity
75 and the presence of frequent endemic species (Torri *et al.*, 2018).

76 They are also relevant from a social and economic point of view. Badlands can be
77 considered aesthetic landscapes, and also magnificent scientific, touristic and
78 educational laboratories for runoff, erosion and vegetation studies at accessible
79 spatial and temporal scales, and for these reasons many researchers suggest that
80 they deserve to be protected (Zgłobicki *et al.*, 2019). Indeed, some badland areas
81 are included within conservation figures such as National Parks or Nature Reserves,
82 and often attract visitors and activities in nature (Torri *et al.*, 2013; Zgłobicki *et al.*,
83 2019). Such activities raise the value of badland areas and encourage local
84 communities to contribute in the preservation of these landscapes.

85 Thereby, research related to badlands has increased progressively throughout the
86 last decades, particularly in the Mediterranean region (Gallart *et al.*, 2013a;
87 Martínez-Murillo and Nadal-Romero, 2018). However, most of these badlands
88 studies have been mainly focused on explaining past and present processes, while
89 the changes expected under future climatic conditions have been hardly analyzed,
90 and present contradictory results.

91 Most of the climate models forecast an increase in temperature and changes in
92 rainfall patterns by the end of the 21st century (Lionello and Scarascia, 2018).
93 However, there is no information about the magnitude and directions of hydro-
94 geomorphological changes in badlands. This lack of knowledge is due to the high
95 uncertainty of the main climatic predictions (Lionello *et al.*, 2014; Vicente-Serrano *et*
96 *al.*, 2020), and the insufficient information about the main climate-drivers controlling
97 the badlands hydro-geomorphological response, and how the effects of these drivers
98 change, as climate does. Changes in temperature and precipitation can critically
99 affect weathering processes, regolith evolution and soil development, hydrological
100 and erosion dynamics, sediment transfer from badland areas to river catchments,

101 and vegetation dynamics. As these processes are interrelated, climate-drivers
102 affecting one of them may have indirect impacts on the others. For example, any
103 climate change that promotes weathering may favor infiltration and would probably
104 increase sediment availability. Thus, it is often difficult to disentangle the direct and
105 independent effects of a climatic driver on a specific hydro-geomorphological
106 process, and the interactions among this process and others also affected by climatic
107 drivers. Structural Equations Models (SEMs) allow us to analyze the complex
108 relationships among different climatic drivers and hydro-geomorphological
109 processes and to separate the direct and indirect effects of these drivers (e.g.
110 Chamizo *et al.*, 2012, 2017; Rodriguez-Caballero *et al.*, 2013, 2014). This provides
111 a more comprehensive picture of the relative importance of these drivers yielding
112 insights into the mechanisms behind their effects and may be very useful in order to
113 understand the magnitude and directions of future hydro-geomorphological changes
114 in badlands, and the resulting on-site and off-site effects in response to changing
115 climatic conditions.

116 One of the regions of the world more prone to suffer intensely the effects of Global
117 Change is the Mediterranean region. Numerous climate studies confirm changes in
118 surface temperature and rainfall patterns (increase in drought frequency and rainfall
119 intensity) (González-Hidalgo *et al.*, 2020; Vicente-Serrano *et al.*, 2020). Besides, this
120 region has a long history of human activity and is densely populated, resulting in land
121 degradation and land cover changes. Thereby, it is expected that the consequences
122 of Global Change will be magnified in this region (Lionello and Scarascia, 2018),
123 causing measurable local impacts with potential regional consequences.

124 Badlands develop within a wide range of climatic environments, especially in the
125 Mediterranean region (Nadal-Romero *et al.*, 2011). The study of badland areas in

126 the Mediterranean region supposes a challenge (numerous complex feedbacks) and
127 an essential target. Mediterranean badlands are subject to dramatic changes that
128 will affect the hydro-geomorphological and vegetation dynamics at different spatial
129 and temporal time-scales (Nadal-Romero *et al.*, 2018a; Rodríguez-Caballero *et al.*,
130 2014). Nevertheless, most of the studies published on Mediterranean badland areas
131 have insufficient temporal length to predict the impacts of Global Change. Despite
132 this is the largest challenge facing future landscapes, there are no prospective
133 analysis on its effects in Mediterranean badlands. This paper aims to gain more
134 insight into the discussion by exploring the following critical research question: What
135 is the fate of Mediterranean badlands under a context of Global Change? To answer
136 it, this study aims at (i) identifying the main climate-drivers affecting the hydro-
137 geomorphological dynamics in a range of climatic environments where
138 Mediterranean badlands develop (from arid to humid areas), and (ii) analyzing how
139 they will change in the future and the likely response of these extraordinary
140 landscapes to Global Change.

141

142 **2. Material and Methods**

143 ***2.1. The Mediterranean region***

144 The Mediterranean region comprises a heterogeneous area around the
145 Mediterranean Sea that stretches c.3,800 km east to west from the tip of Portugal to
146 the shores of Lebanon, and c.1,000 km north to south from Italy to Morocco and
147 Libya (European Commission, 2009), thus encompassing territories from Europe,
148 Africa and Asia. Overall, it is affected by a Mediterranean climate with mild wet
149 winters and warm and hot dry summers. Nonetheless, this general description of the
150 climatic characteristics covers up significant differences, well explained by the

151 heterogeneity of the region itself. Geographical location, orography, humidity and
152 heat supplied by the Mediterranean Sea, are all relevant traits that determine local
153 climatic gradients.

154 Badlands are distributed along the wide variety of climatic conditions that
155 characterize the Mediterranean region. In this study, we use the climatic
156 classification of badlands proposed by Gallart *et al.* (2002), with some small
157 changes, reducing the groups of homogeneous badland types from three to two, due
158 to the scarcity of available data from arid badlands: (i) arid and semiarid (hereafter
159 dry badlands), and (ii) subhumid and humid badlands (hereafter wet badlands).

160 Dry badlands are developed in dryland areas with mean annual rainfall below 700
161 mm. This group includes examples of arid badlands located in the Zin Valley
162 (northern Negev, Israel), characterized for being old landscapes apparently
163 stabilized (mainly by biocrusts) under present climate conditions (Yair *et al.*, 2011,
164 2013) to more active systems, such as Tabernas (Spain) and Basilicata badlands
165 (Italy) (e.g. Brandolini *et al.*, 2018; Calvo and Harvey, 1996; Cantón *et al.*, 2001a,
166 2001b, 2003; Rodríguez-Caballero *et al.*, 2014, 2018a).

167 Wet badlands are very often developed in mountain areas, with mean annual rainfall
168 over 700 mm. They are characterized by extreme hydro-geomorphological dynamics
169 and very high erosion and sediment yields. Some of the best examples are located
170 in the Pyrenees (Spain) (e.g. Gallart *et al.*, 2013b; Llena *et al.*, 2020; Nadal-Romero
171 *et al.*, 2018a) and the sub-Mediterranean Alps (France) (e.g. Mathys *et al.*, 2003).

172

173 **2.2. Data collection and analysis**

174 *2.2.1. Exploring the Mediterranean badlands response along climatic gradients*

175 In a first stage, we performed an exploratory analysis related to the main climate
176 variables (annual rainfall and mean annual temperature) and sediment yield in
177 badland areas, based on the database created by Nadal-Romero *et al.* (2011, 2014).
178 This database included 55 references from 87 study sites including data collected
179 from Morocco, Spain, France, Italy, Albania, Greece, Turkey and Israel. All these
180 studies have information on sediment yield under natural rainfall with a measuring
181 period of at least one year. In addition, in the case of catchments >10ha (considered
182 large in this study), they were only selected when badlands occupied at least 5% of
183 the total catchment.

184 *2.2.2. Analysis of climate-drivers in Mediterranean badland areas*

185 In order to achieve the objective of this manuscript (identifying the main climate-
186 drivers affecting the hydro-geomorphological dynamics in badland areas) the
187 database described by Nadal Romero *et al.* (2011 and 2014) was screened and
188 updated as follows. The study scope was focused on climate factors controlling
189 badlands hydro-geomorphological response from the Mediterranean region. By
190 reading the abstracts and a main body skim reading, the database was screened to
191 identify only relevant studies that described the main climate-drivers controlling
192 badland hydro-geomorphological response (12 manuscripts from the original
193 database) at the catchment scale. Then, a second literature search was performed
194 in Scopus on February 2020 following a systematic literature process according to
195 the guidelines proposed by Mengist *et al.* (2020) as the framework of Search,
196 Appraisal, Synthesis and Analysis (SALSA) (Booth *et al.*, 2012). This new search
197 was restricted to studies published up to 2019, using as key words “Badlands”,
198 “catchment”, and all possible combinations of keywords for hydro-geomorphological
199 response (i.e. [sediment yield, erosion, runoff or weathering]) OR Global Change

200 (i.e. [climate change or Global Change]). We obtained a new set of records to be
201 considered (129 studies). After application of the screening process previously
202 described, 32 studies fulfilled all the inclusion criteria (these were added to the
203 previous database leading to a final database of 44 studies, see Supplementary
204 Table S1).

205 Later, the synthesis stage consisted of extraction and classification of relevant
206 information to identify the main climate-drivers affecting the hydro-geomorphological
207 dynamics of badlands. For each study in the database (see synthesis in Table S1
208 Supplementary Material), the following information was collected (when available):
209 reference, measurement location, climate characteristics (mean annual rainfall and
210 temperature), and main climate-drivers that conditioned the hydro-geomorphological
211 processes (Table 1). For the data analysis stage, we built a driver binary matrix
212 indicating presence or absence of each single driver per study site. From this, we
213 calculated the total number of studies where each driver was reported to have an
214 effect on each study process (weathering, hydrology and erosion). We estimated the
215 relative importance of the different drivers on each single process, as the ratio of the
216 number of studies in which each single driver was reported to the total number of
217 reports for the whole set of drivers. This was done for each single analyzed process,
218 and considering the complete dataset of for dry and wet badlands separately (See
219 Table S1, Supplementary material). Finally, we performed a Non-Metric
220 MultiDimensional Scaling (NMDS) to compare the main drivers acting on each study
221 case within the database.

222 Analysis was performed using the vegan package (Oksanen *et al.*, 2013) in R (R
223 Core Team, 2013). Runs were based on jaccard dissimilarity that well suited to deal
224 with presence-absence binary data. Finally, nonparametric Spearman rank

225 correlations were performed between NMDS axis values and environmental
226 variables to determine how climate-drivers affecting badlands response vary along
227 the temperature and precipitation gradient in which Mediterranean badlands
228 develop.

229 *2.2.3. Analysis of climate-drivers and hydro-geomorphological dynamics interactions*
230 *based on field studies: El Cautivo and Araguás catchments*

231 Weathering, runoff and erosion are interrelated processes, and climate-drivers
232 affecting one of these processes may have indirect impacts on the others.
233 Exploratory analyses based on Structural Equation Models (SEMs) represent a
234 suitable tool to analyse the dependence of one variable on another, as they
235 represent multiple path relationships, and separate direct and indirect effects
236 between predictors. Application of SEMs has shown successful results in a number
237 of hydro-geomorphological studies (e.g. Chamizo *et al.*, 2012, 2017; Rodríguez-
238 Caballero *et al.*, 2013, 2014). Thus, we built a SEM to provide integrated knowledge
239 on the major climatic drivers of badlands hydro-geomorphological response,
240 partitioning causal influences among several variables, and identifying direct and
241 indirect effects of the drivers. This analysis demonstrates how well data support a
242 set of hypothesized direct and indirect relationships among the variables by
243 comparing the covariance structures of model and observed data (Mitchell, 1992;
244 Iriondo *et al.*, 2003; Grace *et al.*, 2010). We hypothesized a priori model based on
245 well-established causal relationships already identified during the review process
246 (Supplementary Figure 1). Model included hydro-geomorphological variables (i.e.
247 runoff rate [RR], runoff coefficient [RC] and maximum peak flows [Q_{max}] and
248 sediment yield [SY]), and the main climate-drivers (rainfall amount [R], maximum
249 rainfall intensity in 5 min [I_{5max}], 3-days antecedent rainfall [R_{-3 days}], and the number

250 of wetting-drying [W-D] and freezing cycles 10 days previous to the event [Fdc] in
251 dry and wet areas, respectively) (see Supplementary Figure 1). As records of these
252 variables in a high number of events was not available for all the study sites included
253 in our database, we restricted the application of the SEM to two study sites, for which
254 long-term event records was available. Thus, this general model was separately
255 tested in two experimental catchments representative of the two groups of
256 Mediterranean badlands, using a high number of stormflow events recorded on each
257 catchment. The two catchments representative of dry and wet badlands were
258 respectively: El Cautivo (number of events: 127) and Araguás (number of events:
259 139) (Cantón *et al.*, 2001a, 2001b; Rodríguez-Caballero *et al.*, 2014; Nadal-Romero
260 *et al.*, 2018a). El Cautivo (Tabernas badlands) is located in SE Spain. The climate
261 is semiarid type, with an average annual temperature of 17.8 °C and an average
262 annual rainfall of 235 mm (for more information see Cantón *et al.*, 2001b, 2003 and
263 Rodríguez-Caballero *et al.*, 2014, 2018a). Runoff and erosion has been measured
264 at this site since 1990 with a H-type flume located at the catchment outlet, which had
265 a contributing area of 1.8 ha. Data corresponding to a period of 20 years was used
266 for running the SEM at this site. The Araguás catchment (45 ha) is located in the
267 Central-Western Pyrenees (NE Spain). The climate is of sub-Mediterranean
268 mountain type, with an average annual temperature of 10 °C and an average annual
269 rainfall of 800 mm (for more information see Nadal-Romero and Regüés, 2010). Data
270 correspond to a period of 14 years was used for running the SEM at this site.

271 Goodness of fit between the empirical and the model-implied covariance matrix was
272 assessed by χ^2 , the Goodness of Fit Index (GFI), the Non-Normed Fit index (NNFI)
273 and the Root Mean Square Error (RMSE). Significant χ^2 values indicate the model
274 does not fit the data, whereas values of GFI and NNFI over 0.9 and RMSE below

275 0.05 indicated the model is good. Finally, we analyzed differences in the climate-
276 drivers controlling hydro-geomorphological response of dry and wet badlands by
277 comparing individual path coefficients between variables obtained with the two
278 different datasets. SEM analysis was done using SPSS AMOS 18 software (AMOS
279 Development Corp., Mount Pleasant, South Carolina, USA).

280 **2.3. Projected climate change scenarios**

281 Based on climate forecasts obtained by the fifth phase Climate Model Inter-
282 Comparison Project (CMIP5), we analyzed expected trends in the main climate-
283 drivers governing the Mediterranean badland dynamics identified in the literature
284 revision and by the SEM analysis. To do this, we obtained information of: (i) mean
285 annual rainfall; (ii) the simple daily intensity index (SDII; Brunetti *et al.*, 2001); (iii)
286 days with rainfall > 1 mm (as a proxy of the number of precipitation events); (iv)
287 number of frost days (defined as the total number of days per year with absolute
288 minimum temperature below 0°C); and (v) water content of the soil layer. The relative
289 change on each driver by the year 2050 (period between 2035 and 2065) relative to
290 historical values (period between 1986 – 2005) was obtained, for the four different
291 representative concentration pathways (RCPs) defined in the CMIP5 (RCP2.6,
292 RCP4.5, RCP6.0 and RCP8.5). Mean daily precipitation and soil moisture content
293 were calculated using the full set of general circulation models considered for the
294 CMIP5 and climate indices (days with rainfall > 1 mm, SDII and the number of frost
295 days) were calculated using the full set of general circulation models considered in
296 the ETCCDI extremes indices archive (Peterson, 2005). All climate predictions were
297 obtained from the KNMI Climate Explorer (<https://climexp.knmi.nl>). Finally, values of
298 specific climate predictions for each study site described in Table S1 was extracted,

299 and this information was used to elucidate the future response of the different
300 badland types.

301 **3. Results and Discussion**

302 **3.1. Climate-drivers in badland areas**

303 Badland hydro-geomorphological functioning has aroused much concern for more
304 than 100 years (Nadal-Romero *et al.*, 2018b). As a result, the main drivers governing
305 badlands response have been identified in different locations around the world (i.e.
306 Boardman *et al.*, 2015; Bollati *et al.*, 2019; Clarke and Rendell, 2010; Yang *et al.*,
307 2019). However, up to now, available datasets did not allow us to analyze how these
308 drivers have varied in response to climate changes and their impacts on badlands
309 hydro-geomorphology, as most of them cover only short periods of time. An
310 extensive literature revision showing badlands erosion rates and the main climate-
311 drivers controlling them, along a climatic gradient, has allowed us to partially filling
312 this gap. As observed in Supplementary Figure 2, erosion rates increased as mean
313 annual rainfall did. Thus, SY was more than 10-fold higher in humid and cold
314 badlands than in arid and semiarid ones. No significant differences have been found
315 between arid and semiarid badlands. These results support our initial classification
316 of Mediterranean badland sites according to the precipitation regime into two main
317 classes: dry badlands and wet badlands. The data also showed a high variability.

318 Differences in SY between dry and wet Mediterranean badlands have been
319 traditionally related to differences in rainfall regime (Gallart *et al.*, 2013a). However,
320 our literature review reveals other important climate-drivers governing the
321 Mediterranean badlands functioning with different relevance in each climatic region
322 (Figure 1; Supplementary Table S1). Figure 1a shows the NMDS ordination of the

323 main climate-drivers for the different analyzed hydro-geomorphological processes
324 (weathering, hydrology or erosion) from the Mediterranean badlands with available
325 data. The study cases appear aligned along a gradient of increasing annual rainfall
326 and decreasing annual temperature, from the lower left side of the plot that included
327 dry badland sites, towards the upper right side of the plot, where wet badlands are
328 located. In addition, the NMDS graph illustrated a clear cluster of the climate-driving
329 factors. Wet badlands tended to group on the upper part of the two-axis plot,
330 associated to drivers such as presence of snow, antecedent moisture, freeze-thaw
331 cycles and total rainfall amount. In contrast, dry badlands grouped at the lower part
332 of the plot being more influenced by rainfall intensity, and timing and seasonality.

333 A deeper analysis of the relative frequency of climatic factors identified as drivers for
334 the main operating processes (weathering, hydrology and erosion) corroborated this
335 overall trend. However, as observed in Figure 1b, the relative importance of the
336 different climatic variables varies depending on the analyzed process and climatic
337 region.

338

339 (i) In **dry** Mediterranean badlands, the main climate-driver is rainfall (magnitude,
340 intensity, and temporal rainfall distribution), although the different studies present
341 some singularities. Wetting-drying cycles appear as the main control for weathering
342 in dry badlands (Figure 1b), triggering physical, chemical and mineralogical changes
343 in the parent material, whose intensity depends on material properties, for instance
344 gypsum, sodium or swelling clay contents (Calvo and Harvey, 1996; Piccarreta *et*
345 *al.*, 2006a; Desir and Marín, 2007, 2013). Although a few wetting-drying cycles are
346 sufficient to induce mineral dissolution, the increase in the number of cycles has
347 been demonstrated to boost weathering processes (Cantón *et al.*, 2001a; Pulice *et*

348 *al.*, 2013). In fact, an increase in weathering rates proportional to the number of
349 rainfall events has been described (Cantón *et al.*, 2001a). Apart from the number of
350 rainfall events, the rainfall amount and the temporal distribution are also important
351 drivers for weathering, modulating the intensity of weathering processes: the higher
352 the rainfall amount, the deeper the physical-chemical-mineralogical alterations
353 (Pulice *et al.*, 2013).

354 Rainfall amount and rainfall intensity are identified as the paramount drivers of runoff
355 generation (Figure 1b). Kuhn *et al.* (2004) and Yair *et al.* (2013) indicated that in arid
356 badlands (Zin Valley), the duration of runoff-effective rainfalls is of critical importance
357 to understand the hydrological dynamics, and only short high intensity rainfalls are
358 effective. These authors suggested that more important than total rainfall is the
359 frequency of individual rainfalls with magnitude sufficient to generate continuous
360 runoff, erosion and sediment export. In general, rainfall thresholds for runoff
361 generation are low, with reported values of 6 mm (Desir and Marín, 2007), 9 mm
362 (Cantón *et al.*, 2001b), 10 mm (Picaretta *et al.*, 2006) or 11 mm (Sirvent *et al.*, 1997)
363 for different dry badlands. Nonetheless, rainfall to runoff is highly variable in each
364 site depending on the rainfall intensity and moisture antecedent conditions (Cantón
365 *et al.*, 2018). As it is revised in different studies (i.e. Cantón *et al.*, 2018) traditionally
366 runoff generation in badland areas was related to infiltration excess surface runoff
367 (related to rainfall variables), but there are other interacting drivers (such as
368 antecedent moisture content), that may influence runoff generation as well,
369 suggesting that other processes (such as saturation excess) due to partial saturation
370 of the soil profile may operate in badland areas.

371 Likewise, both the rainfall amount and intensity also govern the erosion response of
372 dry badlands (Figure 1b) as demonstrated several authors in Tabernas

373 (southeastern Spain), Las Bardenas (northern Spain), and Basilicata and Sicily,
374 (southern Italy) badlands (Brandolini *et al.*, 2018; Calvo-Cases and Harvey, 1996;
375 Cantón *et al.*, 2001b; Desir and Marín, 2013). The rain/drought sequences have also
376 been pointed as a relevant factor affecting geomorphological dynamics, as a
377 consequence of the mentioned influence on weathering processes and
378 consequently on sediment availability (Calvo-Cases and Harvey, 1996), sometimes
379 expressed as the maximum number of consecutive dry and wet days or the mean
380 dry and wet spell days (Piccarreta *et al.*, 2006a). Other studies found that not only
381 was the rainfall intensity a controlling factor on erosion but also the rainfall temporal
382 distribution: soil erosion is mainly triggered during long-lasting dry periods with low-
383 frequency heavy rainfalls (Brandolini *et al.*, 2018). Even though in dry badlands
384 runoff and erosion responses are much more driven by rainfall amount and intensity
385 than by antecedent moisture (Khun *et al.*, 2004; Martínez-Murillo *et al.*, 2013; Yair *et al.*,
386 1980), the effect of this variable can be appreciated at detailed timing (Cantón *et al.*,
387 2001b). In addition, antecedent moisture may affect hydraulic gradient at the start
388 of the rainfall event, affecting sealing and hydrocompaction processes.

389 (ii) In **wet areas**, weathering processes are mainly related to freeze-thaw cycles
390 (frost growing, water availability and cold temperatures in winter) and snow falls and
391 melting, whereas hydrological dynamics are mainly related to total rainfall amount,
392 and erosion dynamics related to rainfall amount and rainfall intensity (Figure 1b).

393 Llena *et al.* (2020) showed that regolith cohesion is significantly correlated with the
394 mean temperature of days below 0 °C (freezing) in the Central Pyrenees. Similar
395 results were observed in other mountain badland areas (Nadal-Romero and Regüés,
396 2010). Decroix and Olivry (2002), in the badlands of the French Southern Alps,
397 concluded that marls are weathered during freeze-thaw cycles, provided that the

398 water content is high enough during winter, identifying 100 cycles or more during
399 one year. Gallart *et al.* (2002) indicated that in wet areas, in contrast with dry
400 badlands, freezing cycles and geliviation processes are much more important than
401 wetting-drying cycles, as it is shown in Figure 1b. Similar results were obtained by
402 Regüés *et al.* (1995), which concluded that the most important physical weathering
403 agents are freezing and frequent freeze-thaw cycles at high moisture levels
404 (although it is only evident in the first 10 cm), suggesting that desiccation plays only
405 a secondary role in physical weathering.

406 Rainfall variables control the hydrological and erosion dynamics of wet badlands
407 (Figure 1b), in accordance with the results obtained in dry badlands. Piqué *et al.*
408 (2014) indicated that runoff in the Central Pyrenees is highly dependent on rainfall
409 and antecedent moisture content. Similar results were also reported for other
410 Mediterranean mountain badlands (López-Tarazón *et al.*, 2010; Nadal-Romero *et al.*
411 *et al.*, 2018a; Tuset *et al.*, 2016). Erosion processes, in general, are a function of rainfall
412 duration, magnitude and intensity (Figure 1b). Descroix and Olivry (2002) indicated
413 that erosion dynamics is mainly controlled by rainfall amount and rainfall intensity
414 and effective rainfall, suggesting that the most erosive events are caused by intense
415 and short rainfalls. Also, Mathys *et al.* (2003) and Bechet *et al.* (2016) indicated that
416 the main climate-driver is rainfall amount (threshold > 9 mm) and rainfall intensity (>
417 60 mm h⁻¹), highlighting the importance of extreme rainfall events. Buendía *et al.*
418 (2016) showed that rainfall intensity together with temperature regime determine
419 erosivity and weathering processes, and thus sediment production. López-Tarazón
420 *et al.* (2009, 2010) concluded that the main drivers are rainfall duration and total
421 rainfall (the longer the duration the higher the sediment yield). In the Western Italian

422 Alps, Bollati *et al.* (2019) also highlighted the importance of drought periods
423 alternating with wet periods and the occurrence of extreme rainfall events.

424 All this together provided an overall picture of the main climate-drivers governing
425 badlands hydro-geomorphological response. However, other factors, such as
426 lithology could also influence the hydro-geomorphological response of badland
427 areas. In that sense, it should be highlighted the important role played by lithology in
428 the rate of weathering in badland areas, regardless of precipitation and temperature.
429 A high number of authors consider lithology “as the main factor controlling badland
430 distribution and morphological diversity under the montane Mediterranean
431 conditions” (Moreno-de las Heras and Gallart, 2016, p. 107) (see also Moreno-de
432 las Heras and Gallart, 2018). Thus, swelling lutites tend to increase in volume during
433 short rainy periods causing bedrock weathering due to repeated wetting-drying
434 cycles, particularly in sub-humid and humid areas. The presence of salts in both
435 lutites and marls also contribute to a rapid and deep bedrock weathering, reducing
436 “the chances for seed germination and plant establishment, particularly in drylands”
437 (Moreno-de las Heras and Gallart, 2018, p. 40). Besides, the presence of
438 exchangeable sodium in lutites enhances the probability of occurrence of clay
439 dispersion, leading to subsurface erosion (García-Ruiz, 2011; Faulkner, 2013;
440 Kasanin-Grubin *et al.*, 2018). Some authors also attributed to well-sorted fine
441 sediments a high probability of disintegration and piping, and ultimately to badland
442 development (Kasanin-Grubin *et al.*, 2018).

443 Likewise, it should be mentioned that the main processes and the effect of climatic
444 drivers varies at different spatial and temporal scales (Nadal-Romero *et al.*, 2011).
445 For example, the influence of drivers affecting weathering processes will be more
446 important for total sediment yield in small catchments than in large areas with

447 numerous sediment sinks. Thus, further research should address the influence of
448 climatic drivers on the operating processes in badlands at different spatial scales
449 (hillslope, micro-catchment, medium and large catchments) and their
450 interconnections over different temporal scales (event, seasonal, intra-annual, inter-
451 annual).

452

453 **3.2. Climate-drivers and hydro-geomorphological dynamics interactions: El** 454 **Cautivo and Araguás catchments**

455 The structural equation modelling presented in Figure 2 provides a comprehensive
456 view of the major climate-drivers controlling the hydro-geomorphological response
457 of two representative sites of dry (El Cautivo, Figure 2a, p-value 0.356 and NFI and
458 GFI > 0.9) and wet (Araguás, Figure 2b, p-value 0.335 and NFI and GFI > 0.9)
459 Mediterranean badlands. These SEM models also allow to assess the relative
460 importance of the climate-drivers (R, I_{5max} , R_{-3day} , and W-D or Fdc) and their
461 interactions on badland runoff and erosion. Testing the direct and indirect
462 relationships between drivers and response variables (RR, RC, Q_{max} and SY) also
463 contribute to disentangle the interactions of weathering, runoff and erosion
464 underlying the functioning of both badlands. A good model fit was obtained in both
465 sites (see Table S2 of the Supplementary material).

466 The SEM explained 57% and 62% of variance in RC and SY, respectively, for El
467 Cautivo site (Figure 2a) and 52% and 59%, respectively, for Araguás site (Figure
468 2b). In both models, R (with the highest effect, see Table S2 Supplementary
469 Material) and I_{5max} showed a significant direct effect on Q_{max} , which in turn had an
470 indirect effect on RC through its direct effect on the increase of RR. Previous studies

471 have also shown that rainfall amount and intensity are the main drivers for Qmax in
472 dry (Cantón *et al.*, 2001b) and wet Mediterranean badlands catchments (Llena *et al.*,
473 2020; Nadal-Romero *et al.*, 2018a). In addition, R-3day exerted a significant direct
474 effect on Qmax at the Araguás catchment (Nadal-Romero *et al.*, 2018a). These
475 results agree with previous studies at this site that support that rainfall characteristic
476 and pre-event conditions (catchment moisture) play an important role in determining
477 the magnitude of the hydrological response (Nadal-Romero *et al.*, 2018a). At both
478 sites, a direct negative effect of I5max on RR was found, attributed to the fact that
479 most intense rainfalls had a short duration and occurred during periods of low
480 antecedent moisture (summer and the beginning of autumn). This produces lower
481 runoff amount than low-intensity but long-lasting rainfalls that fall mainly during the
482 winter season, when antecedent moisture is high and runoff generates rapidly
483 (Chamizo *et al.*, 2012).

484 Rainfall and runoff influenced SY, but with contrasting effects for the dry and the wet
485 catchments. Qmax was the main driver for SY and showed a significant direct effect
486 on SY at both sites (path coefficients of 0.46 and 0.56 for El Cautivo and Araguás,
487 respectively). However, while R-3day had a significant positive effect on SY at El
488 Cautivo, it showed a negative effect at Araguás. This negative effect is mainly
489 explained by the seasonal dynamics observed in the Araguás catchment: high
490 moisture conditions were observed in spring and winter when low SY values were
491 recorded. Thus, sediment transport during spring and winter depended mainly on
492 Qmax, while in summer and autumn on rainfall intensity and Qmax. In El Cautivo,
493 the occurrence of rainfalls large enough to generate runoff are scarce (according to
494 Cantón *et al.* (2001b), only 16% of rainfall exceeded the threshold for runoff
495 generation), being rainfall amount the most important driver for SY (see Table S2

496 Supplementary Material), and I_{5max} was the second one, whose importance was
497 also previously highlighted by Solé-Benet *et al.* (2012) in these badlands.
498 Conversely, for the wet badlands, where R is less constricting, I_{5max} arises as the
499 main climate-driver for SY (Table S2 Supplementary Material), as has been
500 previously reported by Nadal-Romero *et al.* (2018a). Rainfall intensity (I_{5max}) also
501 indirectly influenced SY at both sites through their significant direct effect on Q_{max} .
502 Contrary to expectations, wetting-drying cycles did not exert a significant effect
503 neither on runoff amount nor SY at El Cautivo catchment. At this site, the majority of
504 rainfalls (more than 84%) do not generate runoff but promote sequential wetting-
505 drying cycles able to induce weathering rates of up to $201.47 \text{ t ha}^{-1} \text{ y}^{-1}$. These rates
506 are much higher than the SY rates of $5.3 \text{ t ha}^{-1} \text{ y}^{-1}$ recorded at plot scale on bare
507 marl during the same period (Cantón *et al.*, 2001a, 2001b). Thus, SY in this dry
508 badland system is not limited by weathering but by the occurrence of low-recurrence
509 rainfalls able to generate extreme runoff events and to transport the available
510 sediment (Cantón *et al.*, 2001b). In contrast, at Araguás, Fdc did show a significant
511 direct effect on SY. Detailed studies in the Araguás catchment showed that SY
512 depends on the availability of sediment susceptible to be transported, highlighting
513 the temporal delay between the weathering and erosion processes and sediment
514 transport (Nadal-Romero and Regüés, 2010).

515

516 **3.3. Projected climate changes and its impacts in Mediterranean badland** 517 **dynamics**

518 Climate changes related to hydro-geomorphological processes in the Mediterranean
519 region mainly include changes in temperature and precipitation, the latter being the

520 most direct influencing factor for soil erosion at the global scale (Li and Fang, 2016).
521 Since badlands are very active from a geomorphological point of view, such changes
522 are expected to be highly prominent. The magnitude and direction of changes will
523 depend on the interaction of climate change with soil properties, vegetation cover or
524 land management. Thus, regional differences in this response are expected, and
525 special attention should be paid on how climate-drivers governing the hydro-
526 geomorphological response will be modified in the future. Figures 3, 4 and 5
527 summarize the variations of the most important climate-drivers previously identified
528 (section 3.1) by 2050, according to climate forecast obtained by the CMIP5: (i) mean
529 annual rainfall; (ii) SDII; (iii) days with rainfall > 1 mm (as a proxy of the number of
530 precipitation events); (iv) number of frost days; and (v) water content of the soil layer.

531 An overall decrease in annual rainfall is expected (Figure 3a), affecting almost the
532 entire Mediterranean basin (with some exception in the Alps, where most wet
533 badlands are located). Changes are especially relevant in dry badlands, where a
534 decrease of total rainfall between 3% and 10% of the current value is expected,
535 depending on emissions scenario (Figure 3a; Supplementary Figure 3). Rainfall
536 intensity showed the opposite pattern with an overall increase between 2 and 5%
537 (Figure 3b). This variation could be underestimated if we compared our results with
538 these obtained by regional circulation models which better capture the influence of
539 orography in rainfall, but a similar pattern is expected (Conte et al., 2020). In all
540 scenarios, higher changes are expected in central, northern and southern-Italy, and
541 lower changes are expected in southeastern Spain (Figure 3b; Supplementary
542 Figure 4). Climate-drivers modulating weathering processes will be also affected.
543 For example, as observed in Figure 4, a marked decrease in the number of rainfall
544 (Figure 4a; Supplementary Figure 5) and frost days (Figure 4b; Supplementary

545 Figure 6) is expected by 2050, which may severely affect wetting-drying and freeze-
546 thaw cycles. A substantial decrease in soil moisture, ranging from -2 to -10%, is also
547 projected as a result of the increased temperature and decreased precipitation
548 (Figure 5; Supplementary Figure 7). This decrease, especially relevant in wet
549 badlands, will have direct hydro-geomorphological implications and also some
550 indirect effects.

551 Given the direct relationship between rainfall characteristics and the hydro-
552 geomorphological response (Figures 1 and 2), the slightly decrease in rainfall
553 amount (Figure 3a), and the marked increase in rainfall intensity (Figure 3b) and in
554 the occurrence of more frequent extreme events (Supplementary Figure 8) suggest
555 that badlands will produce lower runoff volumes but greater erosion rates in the near
556 future. However, a general decrease in the number of frost days, number of rainfall
557 events and soil moisture content is expected (Figures 4 and 5). This, together with
558 an increase in temperature and a decrease in the ratio of snow to rain (Navarro-
559 Serrano and López-Moreno, 2017), would reduce weathering processes, sediment
560 availability and subsequent erosion rates, as it is observed and modeled by Clarke
561 and Rendell (2010). Therefore, a future increase of erosion in Mediterranean
562 badlands could be only expected in areas where sediment availability is not limited
563 by weathering dynamics.

564 The reduction in total rainfall and wetting-drying cycles in dry badlands (Figures 3
565 and 4) would lead to a decrease in annual runoff and erosion rates. These
566 predictions fit well with preliminary studies that described a decrease in annual
567 interrill erosion rates in Mediterranean badlands over the last decades (Clarke and
568 Rendell, 2010). However, as observed in Figure 1 and later corroborated by SEM
569 analysis (Figure 2), sediment availability and weathering seem to play only a minor

570 role in dry badlands at the catchment scale. Here, the occurrence of intense rainfalls
571 of magnitude sufficient to connect hillslope runoff to the main channel network seems
572 to be the main driver (Khun *et al.*, 2004; Faulkner, 2008; Godfrey *et al.*, 2008;
573 Rodríguez-Caballero *et al.*, 2014).

574 As both rainfall intensity (Figure 3a) and the occurrence of extreme rainfalls
575 (Supplementary Figure 8) will increase in most dry Mediterranean badlands, higher
576 soil erosion would occur. This will be also enhanced by the expected negative effects
577 that increased aridity, and more prolonged drought periods (Lehner *et al.*, 2006) will
578 play on the scarce plant cover. This will enlarge the size and extent of open areas
579 where runoff is generated. Biological soil crusts, which often cover these open areas
580 will be also negatively affected, conditioning runoff generation, flow connectivity and
581 water erosion in dry badlands (Rodríguez-Caballero *et al.*, 2014, 2018b; Yair *et al.*,
582 2011). Vegetation loss, decrease in biocrust coverage and a replacement of well-
583 developed biocrust communities by early incipient ones will exacerbate interrill
584 erosion and could lead to the formation of rills, increasing flow connectivity
585 (Rodríguez-Caballero *et al.*, 2015) with the consequent increase in SY.

586 Similarly, as observed in dry badlands, most of the forecasted climate-driver
587 changes would reduce weathering processes in wet badlands, due to a decrease in
588 the number of frost days and soil moisture content (Figures 4 and 5). These changes
589 will therefore result in a decrease in sediment supply, and a consequent increase in
590 fluvial erosion because streams tend to scour their channels to compensate the
591 declining sediment arriving from the slopes (e.g. Liébault *et al.*, 2005; Beguería *et*
592 *al.*, 2006; Keesstra, 2007; Sanjuán *et al.*, 2016). Thus, the hydrological responses
593 would be characterized by rapid and intense runoff, but sediment dynamics may be
594 less marked. This fact would enhance a natural revegetation of the slopes and its

595 stabilization. But, what is expected to happen with vegetation dynamics in wet
596 Mediterranean badlands? Current vegetation growth in wet badlands is limited no
597 longer by water availability, as occurs in dry areas (Maestre *et al.*, 2016), but by
598 weathering processes associated to freeze-thaw cycles, particularly on north-facing
599 slopes, and by high erosion rates, preventing the natural regeneration of vegetation
600 (Gallart *et al.*, 2013b; Moreno-de las Heras and Gallart, 2016; Betron *et al.*, 2016;
601 Francke *et al.*, 2018). Climate scenarios and expected hydro-geomorphological
602 dynamics suggest a change in regolith dynamics, allowing the colonization and
603 persistence of well-developed biocrust communities that would contribute to reduce
604 water erosion. A slightly decline in weathering and erosion processes will have an
605 impact on vegetation cover, suggesting that vegetation growing would be enhanced
606 in wet badlands.

607 **3.4. Off-site effects of Mediterranean badland areas under a context of Global** 608 **Change**

609 Badlands are major contributors of sediment to the fluvial network (García-Ruiz *et*
610 *al.*, 2013, 2017). Despite of their small size with regards the total area of river basins
611 (badlands proportion in the catchments with an area $>10^6$ ha is rarely more than 5%,
612 Copard *et al.*, 2018) they provide a significant sediment supply to river networks
613 (14% of the total sediment fluxes in the Rhône River, Copard *et al.*, 2018). Badland
614 contribution to sediment load in Mediterranean areas is even higher, increasing by
615 a factor of 7 to 8 the sediment deliveries (Nadal-Romero *et al.*, 2011). Uber *et al.*
616 (2019) concluded that marly badlands are the main source of suspended sediment
617 for the Caludègne catchment, and Palazón *et al.* (2016) stated that although
618 badlands occupy only 1% of the Barasona reservoir catchment in the Ésera River
619 basin, Spanish Pyrenees, they are the main suspended sediment source for

620 reservoir siltation, reducing rapidly its storage capacity. Thus, any alteration in the
621 badlands hydro-geomorphological functioning, as these expected by Global
622 Change, may have direct impacts on sediment transfer, including channel clogging,
623 alluvial plain dynamics alteration, water quality or reservoir siltation. Moreover,
624 varying sediment supplies/deliveries to the river cause the channel banks to
625 alternate over time between supply-limited and transport-limited situations, leading
626 to an impact on geomorphological evolution of the river channel (Juez *et al.* 2018a).

627 Changes related with badlands sediment supplies have implications in the carbon
628 cycle since sediment traps organic carbon (Battin *et al.*, 2009). Thereby, sediment
629 yield through weathering and erosion processes can be seen as a major contributor
630 to the organic carbon cycle at continental scale (Copard *et al.*, 2007). Recent studies
631 show that the role of badlands in the carbon cycle, as major sediment sources, may
632 depend on the physical and chemical properties of the parent material and on the
633 aggressiveness and duration of the weathering processes (Graz *et al.*, 2012; Copard
634 *et al.*, 2018). Carbon attached to the sediment may ultimately be stored in reservoirs
635 (Schleiss *et al.*, 2016) or can be exported to the oceans (Copard *et al.*, 2018).
636 Unfortunately, the knowledge on the significance of badlands in the carbon cycle at
637 a regional or global scale is still limited (Galy *et al.*, 2015; Copard *et al.*, 2018), and
638 could be modified due to new scenarios proposed by Global Change.

639 Our analysis of the main climate-drivers controlling the response of Mediterranean
640 badlands to Global Change reveals that the hydro-geomorphological off-site effects
641 could be enlarged, with more frequent and intense floods, increased river and
642 reservoir sediment yield, as well as the worsening in the quality of water bodies.
643 Thereby, understanding the current and future sediment supplies from badlands and
644 their role in the carbon cycle is crucial to plan proper adaptation strategies to face

645 the impacts of Global Change. Additionally, this is extremely important in water
646 bodies affected by disturbances in their sediment continuum cycle due to the
647 presence of reservoirs (Schleiss *et al.*, 2016; Juez *et al.*, 2018b, 2018c).

648 We are conscious of the difficulties to project changes for the coming decades in
649 badland areas because of the strong interactions between land use changes and
650 erosion. In general, human activities can induce drastic alterations in rainfall
651 partitioning, soil and plant characteristics, and overland flow. Some badland areas
652 can be subjected to increased human pressure, especially in semiarid regions
653 affected by population growth and grazing in marginal territories. In such cases,
654 pressure over badland regions can increase the already high erosion rates that
655 characterized these systems (e.g. Nadal-Romero *et al.*, 2011) and consequently
656 many efforts should be made to reduce the high rates of sediment yield, although
657 such practices are rarely successful (Nadal-Romero and García-Ruiz, 2018; Rey *et*
658 *al.*, 2003). However, most badlands are affected by an abandonment of grazing,
659 including the surrounding areas, and this should enhance plant recovery in the
660 margins of badlands with the consequent reduction in the access of overland flow
661 into the gullies of the badlands. In any case, this is an extremely complex topic that
662 merits a special scientific focus in the next few years.

663 **4. Conclusions**

664 The hydro-geomorphological response of Mediterranean badlands is strongly
665 affected by climate variables, with different interrelated drivers operating at different
666 temporal and spatial scales in dry and wet regions.

667 Future scenarios for climate-drivers in the Mediterranean region include declining
668 rainfall volumes, and a decrease in the number of frost days and rainfall events, and

669 in soil moisture content, as well as an increase in rainfall intensity. These changes,
670 together with the foreseeable human impact and land cover changes are likely to
671 amplify and modify Mediterranean badland dynamics. The direct and indirect effects
672 of all these drivers interact in a Global Change context to configure an uncertain and
673 complex response of badland systems. Thus, the analysis of the hydro-
674 geomorphological response of badlands to climate change should be done in an
675 overall context that includes, not only the direct effects of climatic drivers on the
676 hydro-geomorphological response, but also all potential indirect interactions
677 between different drivers and processes. Moreover, as the main processes
678 governing hydro-geomorphological response and the influence of climatic drivers on
679 them varies between dry and wet badlands, this should be studied separately. Based
680 on our analysis and interpretations we conclude that:

681 (i) Wetting-drying cycles are the main drivers for weathering in dry
682 badlands, while rainfall amount and rainfall intensity were identified as
683 the main drivers for runoff and erosion, respectively. In dry badlands,
684 the predicted increase in rainfall intensity and frequency of extreme
685 events will lead to an increase in erosion. The expected increase in
686 aridity will have a negative impact on vegetation and biocrust cover,
687 enhancing interrill erosion and overland flow connectivity in the bare
688 areas, eventually emphasizing their off-site effects.

689 (ii) In wet badlands, weathering is controlled by freeze-thaw cycles.
690 Rainfall amount was identified as the main driver for runoff generation,
691 and this together with rainfall intensity were major controlling factors
692 on erosion. Expected climate changes in these badlands suggest that,
693 although the increase in rainfall intensity could increase erosion rates,

694 weathering processes will decline (due to the decrease in the number
695 of frost days and soil moisture contents), as well as runoff volumes,
696 likely having an effect on erosion reduction in the slopes and favoring
697 the stabilization and revegetation of these slopes due to the
698 improvement of the conditions for vegetation growing.

699 Continue monitoring of Mediterranean badland dynamics will be necessary to detect
700 and understand future changes, as well as interdisciplinary teams to work on these
701 complex environments. Control and restoration techniques should be considered as
702 adaptation strategies when important erosion rates occur, taking into account local
703 conditions and future global changes. In badland areas where changes are not
704 expected to be dramatic and with reduced off-site impacts, we propose to protect
705 them as educational hotspots and research laboratories.

706

707 **Acknowledgments**

708 This work was funded by the H2020-MSCA-IF-2018 programme (Marie Skłodowska-
709 Curie Actions) of the European Union under REA grant agreement, number 834329-
710 SEDILAND, the REBIOARID (RTI2018-101921-B-I00) and MANMOUNT (PID2019-
711 105983RB-100/AEI/10.13039/501100011033) projects funded by the Spanish
712 National Plan for Research and the European Union ERDF funds and the RH2O-
713 ARID project (P18-RT-5130) funded by Consejería de Economía, Conocimiento,
714 Empresas y Universidad from the Junta de Andalucía and the European Union
715 ERDF funds. ERC and SC are supported by a HIPATIA-UAL postdoctoral fellowship
716 funded by the University of Almeria.

717

718 **Data Availability Statement**

719 The data that support the findings of this study are available from the corresponding
720 author upon reasonable request.

721

722 **Conflict of interest**

723 The authors declare that they have no conflicts of interest.

724

725 **References**

726 Aucelli PPC, Conforti M, Della Seta M, Del Monte M, D'uva L, Roskopf CM, Vergari
727 F. 2016. Multi-temporal digital photogrammetric analysis for quantitative assessment
728 of soil erosion rates in the Landola catchment of the Upper Orcia Valley (Tuscany,
729 Italy). *Land Degradation & Development* **27**: 1075–1092.

730 Battin T, Luysaert S, Kaplan L, Aufdenkampe AK, Richter A, Tranvik LJ. 2009. The
731 boundless carbon cycle. *Nature Geosciences* **2**: 598–600.

732 Bechet J, Duc J, Loye A, Jaboyedoff M, Mathys N, Malet JP, Klotz S, Le Bouteiller
733 C, Rudaz B, Travelletti J. 2016. Detection of seasonal cycles of erosion processes
734 in a black marl gully from a time series of high-resolution digital elevation models
735 (DEMs). *Earth Surface Dynamics* **4**: 781–798.

736 Beguería S, López-Moreno JI, Gómez-Villar A, Rubio V, Lana-Renault N, García-
737 Ruiz JM. 2006. Fluvial adjustments in the Central Spanish Pyrenees. *Geografiska*
738 *Annaler Series A, Physical Geography* **88**: 177–186.

739 Boardman J, Favis-Mortlock D, Foster I. 2015. A 13-year record of erosion on
740 badland sites in the Karoo, South Africa. *Earth Surface Processes and Landforms*
741 **40**(14): 1964–1981.

742 Bollati IM, Masseroli A, Mortara G, Pelfini M, Trombino L. 2019. Alpine gullies system
743 evolution: erosion drivers and control factors. Two examples from the western Italian
744 Alps. *Geomorphology* **327**: 248–263.

745 Bosino A, Omaran A, Maerker M. 2019. Identification, characterisation and analysis
746 of the Oltrepo Pavese calanchi in the Northern Apennines (Italy). *Geomorphology*
747 **340**: 53–66.

748 Booth A, Sutton A, Papaioannou D. 2012. Systematic Approaches to a Successful
749 Literature Review. SAGE Publications Ltd, Thousand Oaks, CA, USA.

750 Bouachnack H, Sfar Felfoul M, Boussema R, Habib Snane M. 2009. Slope and
751 rainfall effects on the volume of sediment yield by gully erosion in the Souar lithologic
752 formation (Tunisia). *Catena* **78**(2): 170–177.

753 Bouma NA, Imeson AC. 2000. Investigation of relationships between measured field
754 indicators and erosion processes on badland surfaces at Petrer, Spain. *Catena*
755 **40**(2): 147–171.

756 Brandolini P, Pepe G, Capolongo D, Cappadonia C, Cevasco A, Conoscenti C,
757 Marsico A, Vergari F, Del Monte M. 2018. Hillslope degradation in representative
758 Italian areas: Just soil erosion risk or opportunity for development? *Land*
759 *Degradation & Development* **29**: 2050–2068.

760 Breton V, Crosaz Y, Rey F. 2016. Effects of wood chip amendments on the
761 revegetation performance of plant species on eroded marly terrains in a
762 Mediterranean mountainous climate (Southern Alps, France). *Solid Earth* **7**: 599–
763 610.

764 Brunetti M, Maugerib M, Nanni T. 2001. Changes in total precipitation, rainy days
765 and extreme events in northeastern Italy. *International Journal of Climatology* **21**(7):
766 861–871.

767 Bryan RB, Yair A. 1982. *Badland Geomorphology and Piping*. Geo Books, Norwich.
768 408 pp.

769 Buendia C, Vericat D, Batalla RJ, Gibbins CN. 2016. Temporal Dynamics of
770 Sediment Transport and Transient In-channel Storage in a Highly Erodible
771 Catchment. *Land Degradation & Development* **27**(4): 1045–1063.

772 Calvo A, Harvey AM. 1996. Morphology and development of selected badlands in
773 southeast Spain: Implications of climatic change. *Earth Surface Processes and*
774 *Landforms* **21**: 725–735.

775 Cantón Y, Solé-Benet A, Queralt I, Pini R. 2001a. Weathering of a gypsum-
776 calcareous mudstone under semi-arid environment at Tabernas, SE Spain:
777 laboratory and field-based experimental approaches. *Catena* **44**: 111–132.

778 Cantón Y, Domingo F, Solé-Benet A, Puigdefábregas J. 2001b. Hydrological and
779 erosion response of a badlands system in semiarid SE Spain. *Journal of Hydrology*
780 **252**: 65–84.

- 781 Cantón Y, Solé-Benet A, Lázaro R. 2003. Soil-geomorphology relations in
782 gypsiferous materials of the Tabernas Desert (Almería, SE Spain). *Geoderma* **115**:
783 193–222.
- 784 Cantón Y, Rodríguez-Caballero E, Chamizo S, Le Bouteiller C, Solé-Benet A, Calvo-
785 Cases A. 2018. Runoff generation in Badlands. In *Badland Dynamics in the Context*
786 *of Global Change*, Nadal-Romero E, Martínez-Murillo JF, Kuhn NJ (eds). Elsevier:
787 Amsterdam, 155–190 pp.
- 788 Capolongo D, Pennetta L, Piccarreta M, Fallacara G, Boenzi F. 2008. Spatial and
789 temporal variations in soil erosion and deposition due to land-levelling in a semi-arid
790 area of Basilicata (Southern Italy). *Earth Surface Processes and Landforms* **33**: 364–
791 379.
- 792 Chamizo S, Cantón Y, Rodríguez-Caballero E, Domingo F, Escudero A. 2012.
793 Runoff at contrasting scales in a semiarid ecosystem: A complex balance between
794 biological soil crust features and rainfall characteristics. *Journal of Hydrology* **452**-
795 **453**: 130–138.
- 796 Chamizo S, Rodríguez-Caballero E, Roman R, Cantón Y. 2017. Effects of biocrust
797 on soil erosion and organic carbon losses under natural rainfall. *Catena* **148**(2): 117–
798 125.
- 799 Clarke ML, Rendel HL. 2000. The impact of the farming practice of remodeling
800 hillslope topography on badland morphology and soil erosion processes. *Catena*
801 **40**(2): 229–250.

802 Clarke ML, Rendel HL. 2006. Process-form relationships in Southern Italian
803 badlands: erosion rates and implications for landform evolution. *Earth Surface*
804 *Processes and Landforms* **31**(1): 15–29.

805 Clarke ML, Rendel HL. 2010. Climate-driven decrease in erosion in extant
806 Mediterranean badlands. *Earth Surface Processes and Landforms* **35**: 1281–1288.

807 Conte D, Gualdi S, Lionello P. 2020. Effect of model resolution on intense and
808 extreme precipitation in the Mediterranean region. *Atmosphere* **11**(7): 699.

809 Copard Y, Amiotte-Suchet P, Di-Giovanni C. 2007. Storage and release of fossil
810 organic carbon related to weathering of sedimentary rocks. *Earth and Planetary*
811 *Science Letters* **258**: 345–357.

812 Copard Y, Eyrolle F, Radakovitch O, Poirel A, Rimbault P, Gairoard S, Di-Giovanni
813 C. 2018. Badlands as a hotspot of petrogenic contribution to riverine particulate
814 organic carbon to the Gulf of Lion (NW Mediterranean Sea). *Earth Surface*
815 *Processes and Landforms* **43**: 2495–2509.

816 Crosaz Y, Dinger F. 1999. Mesure de l'érosion sur ravines élémentaires et essais
817 de végétalisation. Bassin versant expérimental de Draix. In *Les bassins versants*
818 *expérimentaux de Draix laboratoire d'étude de l'érosion en montagne-actes du*
819 *séminaire, Draix Le Brusquet Digne, Cemagref (Eds.), 103–118 pp.*

820 Della Seta M, Del Monte M, Fredi P, Lupia Palmieri E. 2009. Space-time variability
821 of denudation rates at the catchment and hillslope scales on the Tyrrhenian side of
822 Central Italy. *Geomorphology* **107**: 161–177.

823 Descroix L, Olivry JC. 2002. Spatial and temporal factors of erosion by water of black
824 marls in the badlands of the French southern Alps. *Hydrological Sciences-Journal-
825 des Sciences Hydrologiques* **47**(2): 227–242

826 Desir G, Marín C. 2007. Factors controlling the erosion rates in a semi-arid zone
827 (Bardenas Reales, NE Spain). *Catena* **71**: 31–40.

828 Desir G, Marín C. 2013. Role of erosion processes on the morphogenesis of a
829 semiarid badland area. Bardenas Reales (NE Spain). *Catena* **106**: 83–92.

830 European Commission, 2009. Natura 2000 in the Mediterranean Region. European
831 Commission Environmental Directorate General.

832 Fairbridge RW. 1968. *Encyclopedia of Geomorphology*. Reinhold Book Corp., New
833 York. 1295 pp.

834 Faulkner H. 2008. Connectivity as a crucial determinant of badland morphology and
835 evolution. *Geomorphology* **100**(1-2): 91–103.

836 Faulkner H. 2013. Badlands in marl lithologies: a field guide to soil dispersion,
837 subsurface erosion and piping-origin gullies. *Catena* **106**: 42–53.

838 Francke T, Foerster S, Brosinsky A, Sommerer E, López-Tarazón JA, Güntner A,
839 Batalla RJ, Bronstert A. 2018. Water and sediment fluxes in Mediterranean
840 mountainous regions: comprehensive dataset for hydro-sedimentological analyses
841 and modelling in a mesoscale catchment (River Isábena, NE Spain). *Earth System
842 Science Data* **10**: 1063–1075.

843 Gallart F, Solé A, Puigdefábregas J, Lázaro R. 2002. Badland systems in the
844 Mediterranean. In *Dryland rivers: Hydrology and Geomorphology of Semi-arid*
845 *Channels*, Bull JL, Kirkby MJ (eds). Wiley. Chichester pp. 299–326.

846 Gallart F, Marignani M, Pérez-Gallego N, Santi E, Macherini S. 2013a. Thirty years
847 of studies on badlands, from physical to vegetational approaches. A succinct review.
848 *Catena* **106**: 4–11.

849 Gallart F, Pérez-Gallego N, Latron J, Catari G, Martínez-Carreras N, Nord G. 2013b.
850 Short- and long-term studies of sediment dynamics in a small humid mountain
851 Mediterranean basin with badlands. *Geomorphology* **196**: 242–251.

852 Galy V, Peucker-Ehrenbrink B, Eglinton T. 2015. Global carbon export from the
853 terrestrial biosphere controlled by erosion. *Nature* **521**: 204–207.

854 García-Ruiz JM. 2011. Una revisión de los procesos de sufosión o piping en España.
855 *Cuadernos de Investigación Geográfica* **37**(1): 7–24.

856 García-Ruiz JM, Nadal-Romero E, Lana-Renault N, Beguería S. 2013. Erosion in
857 Mediterranean landscapes: Changes and future challenges. *Geomorphology* **198**:
858 20–36.

859 García-Ruiz JM, Beguería S, Lana-Renault N, Nadal-Romero E, Cerdà A. 2017.
860 Ongoing and emerging questions in water erosion studies. *Land Degradation &*
861 *Development* **28**: 5–21.

862 Godfrey AE, Everitt BL, Martín-Duque JF. 2008. Episodic sediment delivery and
863 landscape connectivity in the mancos Shale badlands and Fremont River system,
864 Utah, USA. *Geomorphology* **102**(2): 242–251.

865 González-Hidalgo JC, Peña-Angulo D, Beguería S, Brunetti M. 2020. MOTEDAS
866 century: A new high-resolution secular monthly maximum and minimum temperature
867 grid for the Spanish mainland (1916–2015). *International Journal of Climatology*.
868 DOI: 10.1002/joc.6520

869 Grace JB, Anderson TM, Olf H, Scheiner SM. 2010. On the specification of
870 structural equation models for ecological systems. *Ecological Monographs* **80**(1):
871 67–87.

872 Graz Y, Di-Giovanni C, Copard Y, Mathys N, Cras A, Marc V. 2012. Annual fossil
873 organic carbon delivery due to mechanical and chemical weathering of marly
874 badlands areas. *Earth Surface Processes and Landforms* **37**: 1263–1271.

875 Guardià R, Gallart F, Ninot JM. 2000. Soil seed bank and seedling dynamics in
876 badlands of the Upper Llobregat basin (Pyrenees). *Catena* **40**: 189–202.

877 Iriondo JM, Albert MJ, Escudero A. 2003. Structural equation modelling: An
878 alternative for assessing causal relationships in threatened plant populations.
879 *Biological Conservation* **113**(3): 367–277.

880 Juez C, Hassan MA, Franca MJ. 2018a. The origin of fine sediment determines the
881 observations of suspended sediment fluxes under unsteady flow conditions. *Water*
882 *Resources Research* **54**: 5654–5669.

883 Juez C, Bühlmann I, Maechler G, Schleiss AJ, Franca MJ. 2018b. Transport of
884 suspended sediments under the influence of bank macro-roughness. *Earth Surface*
885 *Processes and Landforms* **43**: 271–284.

886 Juez C, Thalmann M, Schleiss AJ, Franca MJ. 2018c. Morphological resilience to
887 flow fluctuations of fine sediment deposits in bank lateral cavities. *Advances in Water*
888 *Resources* **115**: 44–59.

889 Kasanin-Grubin M, Bryan R. 2007. Lithological properties and weathering response
890 on badland hillslopes. *Catena* **70**(1): 68–78.

891 Kasanin-Grubin M, Vergari F, Troiani, F, Della Seta M. 2018. The role of lithology:
892 Parent material controls on badland development. In *Badland Dynamics in the*
893 *Context of Global Change*, Nadal-Romero E, Martínez-Murillo JF, Kuhn NJ (eds).
894 Elsevier: Amsterdam, pp. 61–109.

895 Keesstra, SD, Impact of natural reforestation on floodplain sedimentation in the
896 Dragonja basin, SW Slovenia. *Earth Surface Processes and Landforms* **32**: 49–65.

897 Kuhn N, Yair A. 2004. Spatial distribution of surface conditions and runoff generation
898 in small arid watersheds, Zin Valley Badlands, Israel. *Geomorphology* **57**(3-4): 183–
899 200.

900 Kuhn N, Yair A, Kasanin Grubin M. 2004. Spatial distribution of surface properties,
901 runoff generation and landscape development in the Zin Valley Badlands, northern
902 Negev, Israel. *Earth Surface Processes and Landforms* **29**: 1417–1430.

903 Lehner B, Döll P, Alcamo J, Henrichs T, Kaspar F. 2006. Estimating the impact of
904 global change on flood and drought risks in Europe: a continental, integrated
905 analysis. *Climatic Change* **75**(3): 273–299.

906 Li Z, Fang H. 2016. Impacts of climate change on water erosion: A review. *Earth-*
907 *Science Reviews* **163**: 94–117.

908 Liébault F, Gómez B, Page M, Marden M, Peacock D, Richard D, Trotter CM. 2005.
909 Land-use change, sediment production and channel response in upland regions.
910 *River Research and Applications* **21**: 739–756.

911 Lionello P, Abrantes F, Gacic M, Planton S, Trigo R, Ulbrich U. 2014. The climate of
912 the Mediterranean region: research progress and climate change impacts. *Regional*
913 *Environmental Change* **14**: 1679–1684.

914 Lionello P, Scarascia L. 2018. The relation between climate change in the
915 Mediterranean region and global warming. *Regional Environmental Change* **18**(5):
916 1481–1493.

917 Llena M, Smith MW, Weathon JM, Vericat D. 2020. Geomorphic process signatures
918 reshaping sub-humid Mediterranean badlands: 2. Application to 5-year dataset.
919 *Earth Surface Processes and Landforms* **45**(5): 1292–1310.

920 López-Tarazón JA, Batalla RJ, Vericat D, Francke T. 2009. Suspended sediment
921 transport in a highly erodible catchment: The River Isábena (Southern Pyrenees).
922 *Geomorphology* **109**: 210–221.

923 López-Tarazón JA, Batalla RJ, Vericat D, Balasch JC. 2010. Rainfall, runoff and
924 sediment transport relations in a mesoscale mountainous catchment: The River
925 Isábena (Ebro basin). *Catena* **82**: 23–34.

926 Maestre FT, Eldridge DJ, Soliveres S, Kéfi S, Delgado-Baquerizo M, Bowker MA,
927 García-Palacios P, Gaitán J, Gallardo A, Lázaro R, Berdugo M. 2016. Structure and
928 functioning of dryland ecosystems in a changing world. *Annual Review of Ecology,*
929 *Evolution and Systematics* **47**: 215–237

930 Martínez-Casasnovas JA, Antón-Fernández C, Ramos MC. 2003. Sediment
931 production in large gullies of the Mediterranean area (NE Spain) from high-resolution
932 digital elevation models and geographical information systems analysis. *Earth*
933 *Surface Processes and Landforms* **28**: 443–456.

934 Martínez-Casasnovas JA, Ramos MC, Poesen J. 2004. Assessment of sidewall
935 erosion in large gullies using multi-temporal DEMs and logistic regression analysis.
936 *Geomorphology* **58**: 305–321.

937 Martínez-Murillo JF, Nadal-Romero E, Regüés D, Cerdà A, Poesen J. 2013. Soil
938 erosion and hydrology of the western Mediterranean badlands throughout rainfall
939 simulation experiments: A review. *Catena* **106**: 101–112.

940 Martínez-Murillo JF, Nadal-Romero E. 2018. Perspectives on Badland Studies in the
941 Context of Global Change. In *Badland Dynamics in the Context of Global Change*,
942 Nadal-Romero E, Martínez-Murillo JF, Kuhn NJ (eds). Elsevier: Amsterdam, pp. 1–
943 25.

944 Mathys N, Brocot S, Meunier M, Richard D. 2003. Erosion quantification in the small
945 marly experimental catchments of Draix (Alpes de Haute Provence, France).
946 Calibration of the ETC rainfall-runoff-erosion model. *Catena* **50**: 527–548.

947 Mengist W, Soromessa T, Legese G. 2020. Method for conducting systematic
948 literature review and meta-analysis for environmental science research. *MethodsX*
949 **7**: 100777.

950 Mitchell RJ. 1992. Testing evolutionary and ecological hypotheses using path
951 analysis and structural equation modelling. *Functional Ecology* **6**(2): 123–129.

952 Moreno-de las Heras M, Gallart F. 2016. Lithology controls the regional distribution
953 and morphological diversity of montane Mediterranean badlands in the upper
954 Llobregat basin (eastern Pyrenees). *Geomorphology* **271**: 107–115.

955 Moreno-de las Heras M, Gallart F. 2018. The origin of badlands. In *Badland*
956 *dynamics in the context of Global Change*, Nadal-Romero E, Martínez-Murillo JF,
957 Kuhn N.J. (eds.). Elsevier: Amsterdam, pp. 217–253.

958 Nadal-Romero E, García-Ruiz JM. 2018. Rethinking spatial and temporal variability
959 of erosion in badlands. In *Badland Dynamics in the Context of Global Change*,
960 Nadal-Romero E, Martínez-Murillo JF, Kuhn NJ (eds). Elsevier: Amsterdam pp. 217–
961 253.

962 Nadal-Romero E, Regüés D. 2010. Geomorphological dynamics of sub-humid
963 mountain badland areas: weathering, hydrological and suspended sediment
964 transport processes. A case of study in the Araguás catchment (Central Pyrenees),
965 and implications for altered hydro-climatic regimes. *Progress in Physical Geography*
966 **34**(3): 123–150.

967 Nadal-Romero E, Martínez-Murillo JF, Vanmaercke M, Poesen J. 2011. Scale-
968 dependency of sediment yield from badland areas in Mediterranean environments.
969 *Progress in Physical Geography* **35**(3): 297–332.

970 Nadal-Romero E, Martínez-Murillo JF, Vanmaercke M, Poesen J. 2014.
971 Corrigendum to “Scale-dependency of sediment yield from badland areas in
972 Mediterranean environments” (*Progress in Physical Geography* 35 (3) (2011) 297-
973 332). *Progress in Physical Geography* **38**(3): 381–386.

974 Nadal-Romero E, Martínez-Murillo JF, Khun NJ. 2018b. *Badland dynamics in the*
975 *context of Global Change*. Elsevier, Amsterdam, 320 pp.

976 Nadal-Romero E, Peña-Angulo D, Regüés D. 2018a. Rainfall, runoff and sediment
977 transport dynamics in a humid mountain badland area: long-term results from a small
978 catchment. *Hydrological Processes* **32**: 1588–1606.

979 Navarro-Serrano F, López-Moreno JI. 2017. Spatio-temporal analysis of snowfall
980 events in the Spanish Pyrenees and their relationship to atmospheric circulation.
981 *Cuadernos de Investigación Geográfica* **43**(1): 233–245.

982 Oksanen J, Guillaume Blanchet F, Kindt R, Legendre P. et al. 2013. Vega:
983 community ecology package. [http://cran.r-](http://cran.r-project.org/web/packages/vegan/vegan.pdf)
984 [project.org/web/packages/vegan/vegan.pdf](http://cran.r-project.org/web/packages/vegan/vegan.pdf)

985 Palazón L, Latorre B, Gaspar L, Blake WH, Smith HG, Navas A. 2016. Combining
986 catchment modelling and sediment fingerprinting to assess sediment dynamics in a
987 Spanish Pyrenean river system. *Science of the Total Environment* **569-570**: 1136–
988 1148.

989 Peterson TC. 2005. Climate Change Indices. *WMO Bulletin* **54**(2): 83–86.

990 Piccarreta M, Faulkner H, Bentivenga M, Capolongo D. 2006a. The influence of
991 physico-chemical material properties on erosion processes in the badlands of
992 Basilicata, Southern Italy. *Geomorphology* **81**(3-4): 235–251.

993 Piccarreta M, Capolongo D, Boenzi F, Bentivenga M. 2006b. Implications of decadal
994 changes in precipitation and land use policy to soil erosion in Basilicata, Italy. *Catena*
995 **65**: 138–151.

996 Pimentel D, Harvey C, Resosudarmo P, Sinclair K, Kurz D, McNair M, Crist S, Shpritz
997 L, Fitton L, Saffouri R, Blair R. 1995. Environmental and economic costs of soil
998 erosion and conservation benefits. *Science* **267**(5201): 1117–1123.

999 Piqué G, López-Tarazón JA, Batalla RJ. 2014. Variability of in channel sediment
1000 storage in a river draining highly erodible areas (the Isábena, Ebro Basin). *Journal*
1001 *of Soils and Sediments* **14**: 2031–2044.

1002 Pulice I, Di Leo P, Robustelli G, Scarciglia F, Cavalcante F, Belsivo C. 2013. Control
1003 of climate and local topography on dynamics evolution of badland from southern Italy
1004 (Calabria). *Catena* **109**: 83–95.

1005 Regüés D, Pardini G, Gallart F. 1995. Regolith behaviour and physical weathering
1006 of clayey mudrock as dependent on seasonal weather conditions in a badland area
1007 at Vallcebre, Eastern Pyrenees. *Catena* **25**: 199–212.

1008 Regüés D, Guàrdia R, Gallart F. 2000. Geomorphic agents versus vegetation
1009 spreading as causes of badland occurrence in a Mediterranean subhumid
1010 mountainous area. *Catena* **20**: 173–187.

1011 Rey F. 2003. Influence of vegetation distribution on sediment yield in forested marly
1012 gullies. *Catena* **50**: 549–562.

1013 Rey F. 2009. A strategy for fine sediment retention with bioengineering works in
1014 eroded marly catchments in a mountainous Mediterranean climate (southern Alps,
1015 France). *Land Degradation & Development* **20**: 210–216.

1016 Ries F, Schmidt S, Sauter M, Lange J. 2017. Controls of runoff generation along a
1017 steep climatic gradient in the Eastern Mediterranean. *Journal of Hydrology: Regional*
1018 *Studies* **9**: 18–33.

- 1019 Rodríguez-Caballero E, Cantón Y, Lázaro R, Solé-Benet A. 2014. Cross-scale
1020 interactions and nonlinearities in the hydrological and erosive behaviour of semiarid
1021 catchments: the role of biological soil crusts. *Journal of Hydrology* **57**: 815–825.
- 1022 Rodríguez-Caballero E, Cantón Y, Jetten V. 2015. Biological soil crust effects must
1023 be included to accurately model infiltration and erosion in drylands: An example from
1024 Tabernas Badlands. *Geomorphology* **241**: 331–342.
- 1025 Rodríguez-Caballero E, Lázaro R, Cantón Y, Puigdefábregas J, Solé-Benet A.
1026 2018a. Long-term hydrological monitoring in arid-semiarid Almería, SE Spain. What
1027 have we learned? *Cuadernos de Investigación Geográfica* **44**(2): 581–600.
- 1028 Rodríguez-Caballero E, Chamizo S, Roncero-Ramos B, Román R, Cantón Y. 2018b.
1029 Runoff from biocrust: A vital resource for vegetation performance on Mediterranean
1030 steppes. *Ecohydrology* **11**(6): e1977
- 1031 Rodríguez-Caballero E, Román JR, Chamizo S, Roncero Ramos B, Cantón Y. 2019.
1032 Bicrust landscape-scale spatial distribution is strongly controlled by terrain attributes:
1033 Topographic thresholds for colonization in a Semiarid Badland System. *Earth*
1034 *Surface Processes and Landforms* **44**(14): 2771–2779.
- 1035 Sanjuán Y, Gómez-Villar A, Nadal-Romero E, Álvarez-Martínez J, Arnáez J,
1036 Serrano-Muela MP, Rubiales JM, González-Sampériz P, García-Ruiz JM. 2016.
1037 Linking land cover changes in the sub-alpine and montane belts to changes in a
1038 torrential river. *Land Degradation & Development* **27**: 179–189.
- 1039 Schleiss AJ, Franca MJ, Juez C, De Cesare G. 2016. Reservoir Sedimentation.
1040 *Journal of Hydraulic Research* **54**: 595–614.

- 1041 Sirvent J, Desir G, Gutiérrez M, Sancho C, Benito G. 1997. Erosion rates in badland
1042 areas recorded by collectors, erosion pins and profilometer techniques (Ebro Basin
1043 NE-Spain). *Geomorphology* **18**: 61–75.
- 1044 Solé-Benet A, Afana A, Cantón Y. 2012. Erosion pins, profile and laser scanners for
1045 soil erosion monitoring in active hillslopes in badlands of SE Spain. In *Actas XII*
1046 *Reunión Nacional de Geomorfología*, Santander, 575–578 pp.
- 1047 Torri D, Santi E, Marignani M, Rossi M, Borselli L, Maccherini S. 2013. The recurring
1048 cycles of biancane badlands: erosion, vegetation and human impact. *Catena* **106**:
1049 22–30.
- 1050 Torri D, Rossi M, Brogi F, Marignani M, Bacaro G, Santi E, Tordoni E, Amici V,
1051 Maccherini S. 2018. Badlands and the dynamics of human history, land use, and
1052 vegetation through centuries. In *Badland Dynamics in the Context of Global Change*,
1053 Nadal-Romero E, Martínez- Murillo JF, Kuhn NJ (eds). Elsevier: Amsterdam, pp.
1054 111–153.
- 1055 Tuset J, Vericat D, Batalla RJ. 2016. Rainfall, runoff and sediment transport in a
1056 Mediterranean mountainous catchment. *Science of the Total Environment* **540**: 114–
1057 132.
- 1058 Uber M, Legout C, Nord G, Crouzet C, Demory F, Poulenard J. 2019. Comparing
1059 alternative tracing measurements and mixing models to fingerprint suspended
1060 sediment sources in a mesoscale Mediterranean catchment. *Journal of Soils and*
1061 *Sediments* **19**: 3255–3273.
- 1062 Vicente-Serrano SM, McVicar TR, Miralles DG, Yang Y, Tomas-Burguera M. 2020.
1063 Unraveling the influence of atmospheric evaporative demand on drought and its

1064 response to climate change. *Wiley Interdisciplinary Reviews: Climate Change* **11**(2):
1065 e632.

1066 Yair A, Lavee H, Bryan RB, Adar E. 1980. Runoff and erosion processes and rates
1067 in the Zin Valley, Northern Negev, Israel. *Earth Surface Processes and Landforms*
1068 **6**(3): 205–225.

1069 Yair A, Almog R, Veste M. 2011. Differential hydrological response of biological
1070 topsoil crusts along a rainfall gradient in a sandy arid area: Northern Negev desert,
1071 Israel. *Catena* **87**(3): 326–333.

1072 Yair A, Bryan A, Lavee H, Schwanghart W, Kuhn N. 2013. The resilience of a
1073 badland area to climate change in an arid environment. *Catena* **106**: 12–21.

1074 Yang CJ, Yeh LW, Cheng YC, Jen CH, Lin J. 2019. Badland erosion and its
1075 morphometric features in the tropical monsoon area. *Remote Sensing* **11**(24): 3051.

1076 Zglobicki W, Poesen J, Cohen M, Del Monte M, García-Ruiz JM, Ionita L, Niacsu L,
1077 Machová Z, Martín-Duque JF, Nadal-Romero E, Pica A, Rey F, Solé-Benet A,
1078 Stankoviansky M, Stolz Ch, Torri D, Soms J, Vergari F. 2019. The potential of
1079 permanent gullies in Europe as geomorphosites. *Geoheritage* **11**: 217–239.

Figure 1. (a) Non-metric MultiDimensional Scaling (NMDS) ordination of the main hydro-geomorphological drivers from the different Mediterranean badlands. (b) Weight Relative importance of different identified climate-drivers (Rainfall amount, Rainfall intensity, Timing/Seasonality, Wetting-drying cycles, Freeze-thawing cycles, Antecedent soil moisture and Snow) for the main operating processes in badlands (weathering, hydrology, and erosion) in dry (arid, semiarid and dry subhumid) and wet (subhumid and humid) badlands. (data presented in supplementary Table S1).

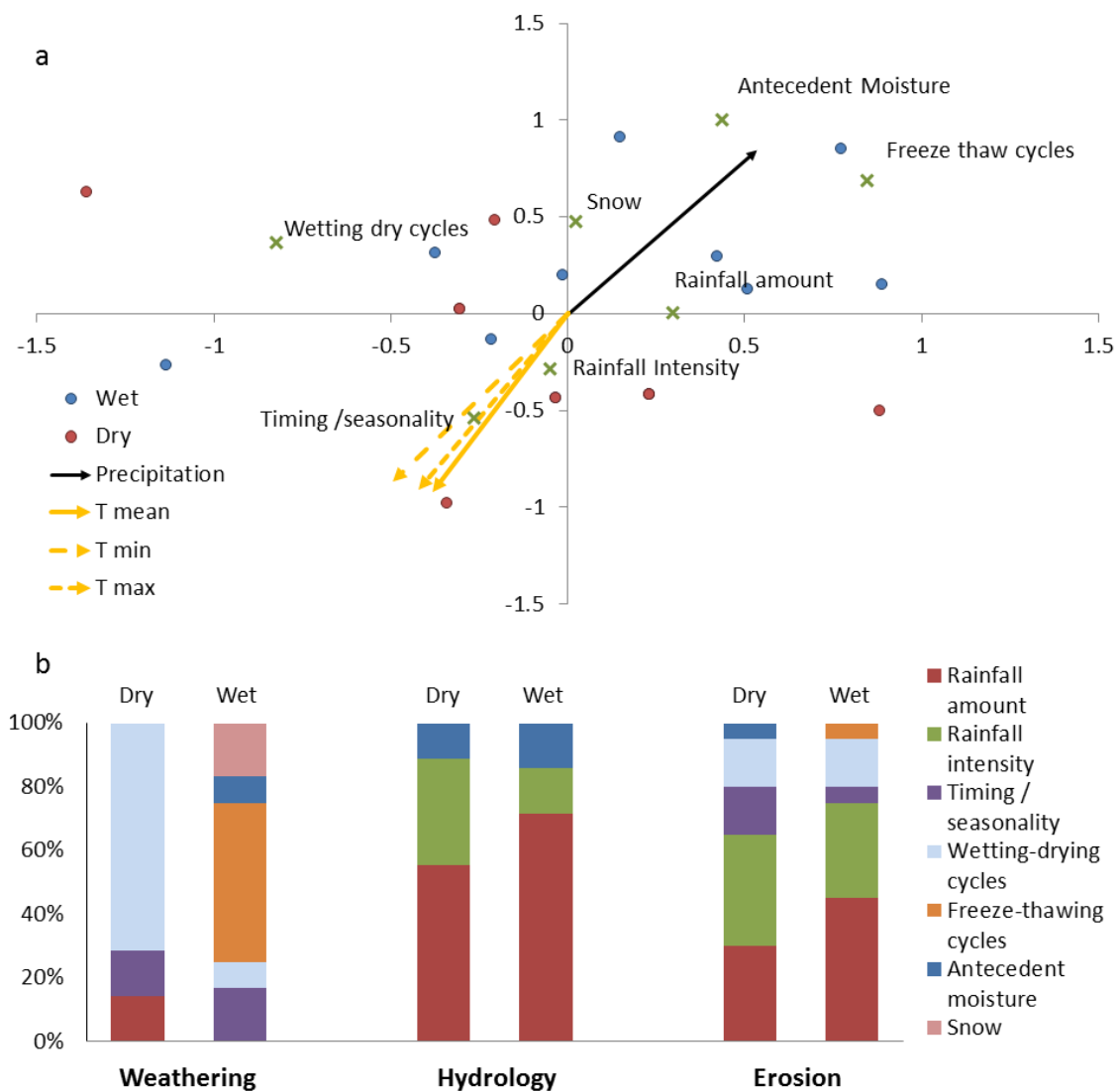
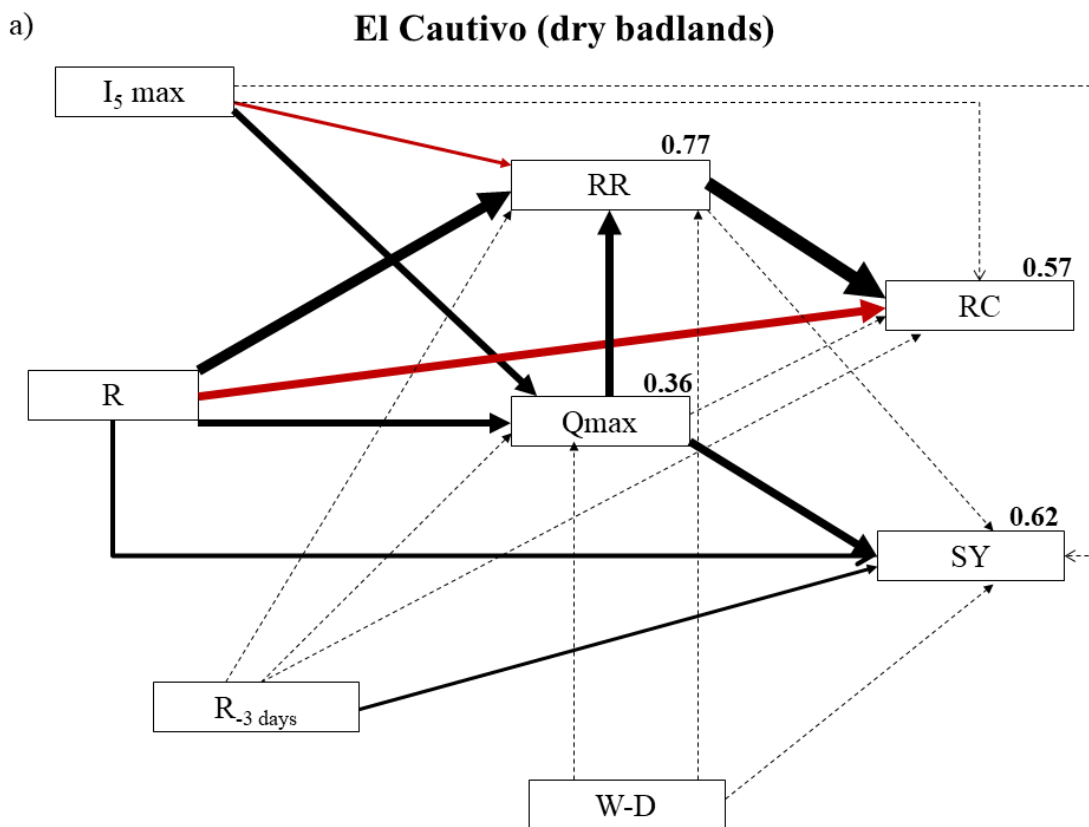


Figure 2. Figure 2. Structural equation models (SEM models) showing the relationships between the significant climate-drivers (Rainfall amount [R], maximum rainfall intensity in 5 min [I5max], 3-days antecedent rainfall [R-3 days], and the number of wetting-drying [W-D] and freezing cycles 10 days previous to the event [Fdc]) and the runoff (runoff rate [RR], runoff coefficient [RC] and maximum peak flows [Qmax]) and erosion response (sediment yield , [SY]) in the two study cases: (a) El Cautivo (dry badlands) and (b) Araguás (wet badlands). Both models showed a good fit with p values of 0.357 and 0.335, respectively, and NFI and GFI over 0.9. The number in bold represents the explained variance of dependent variables. Arrow widths are proportional to the magnitude of standardized path coefficients. Black and red arrows indicate positive and negative effects, respectively. Dash lines indicate non-significant paths ($p > 0.05$). (Rainfall amount [R], maximum rainfall intensity in 5 min [I5max], 3-days antecedent rainfall [R-3 days], and the number of wetting-drying [W-D] and freezing cycles 10 days previous to the event [Fdc]).



b)

Araguás (wet badlands)

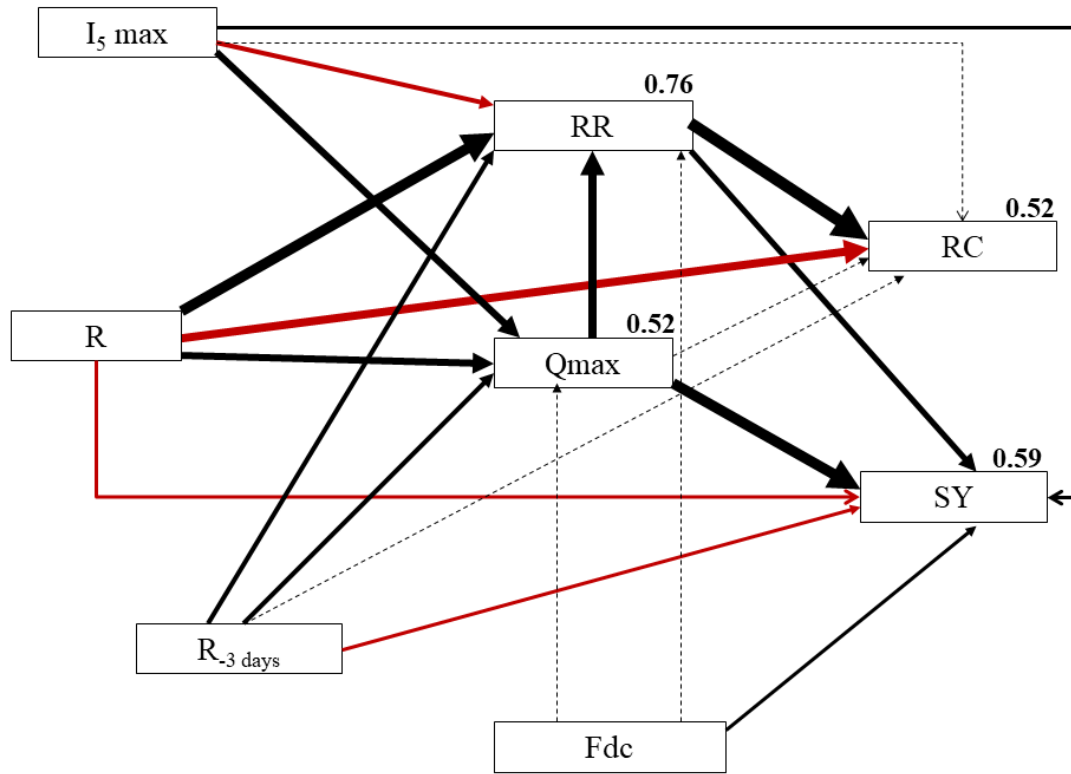


Figure 3. (a) Expected change in mean annual rainfall (mm d^{-1} /year) and (b) simple daily intensity index (SDII; mm/day) in the Mediterranean basin according to the RCP4.5 of the fifth phase Climate Model Inter-Comparison P. Right plot shows the mean changes (%) based on present values for dry (red) and wet (blue) badlands, including four RCPs. Red circles: dry badlands; blue circles: wet badlands. Maps showing expected changes in mean annual rainfall and SDII for RCP2.6, RCP6.0 and RCP8.5 are shown in Supplementary Figures 3 and 4, respectively.

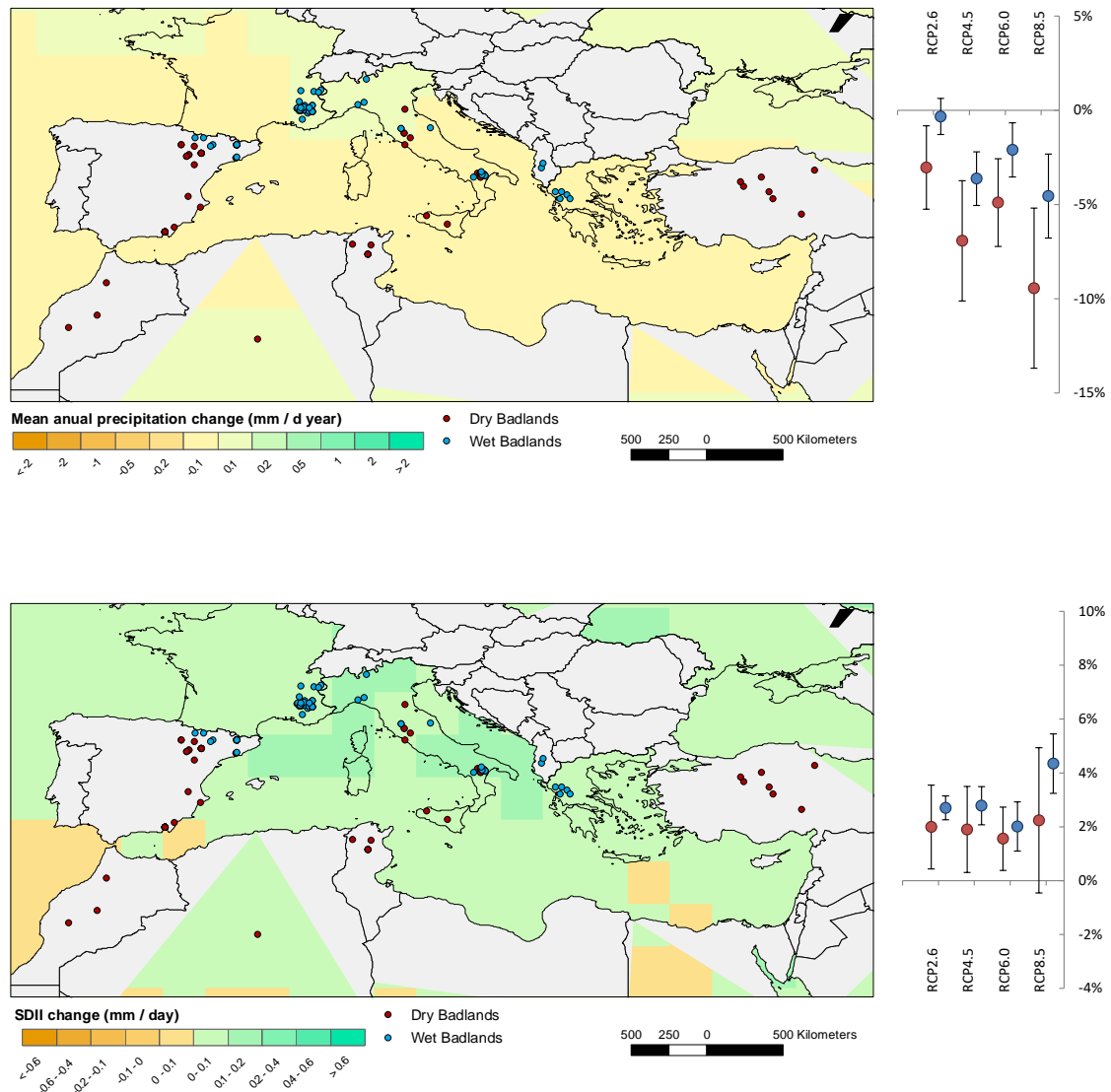


Figure 4. (a) Expected change in the number of precipitation events (number of days with total rainfall > 1mm) and (b) number of frost days (number of days with mean temperature < 0°) in the Mediterranean basin according to the RCP4.5 of the fifth phase Climate Model Inter-Comparison Project (change in 2050 compared to 2005). Right plot shows the mean changes (%) based on present values for dry (red) and wet (blue) badlands, including four RCPs scenarios. Maps showing expected changes in the number of precipitation events and frost days for RCP2.6, RCP6.0 and RCP8.5 are shown in Supplementary Figures 5 and 6, respectively.

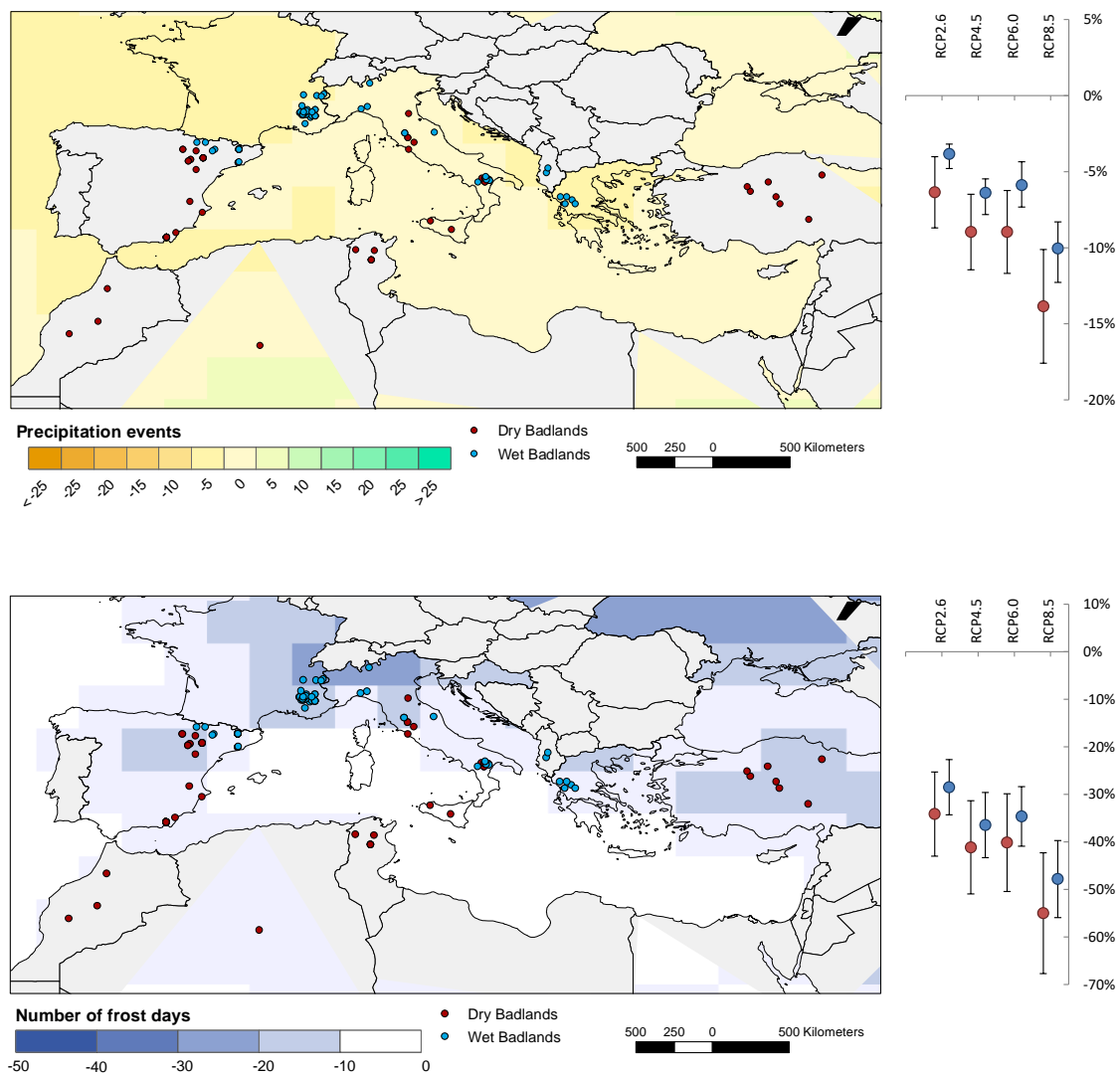


Figure 5. Expected change moisture content of the soil layer (kg m^{-2}) in the Mediterranean basin according to the RCP4.5 of the fifth phase Climate Model Inter-Comparison Project (change in 2050 compared to 2005). Right plot shows the mean changes (%) based on present values for dry (red) and wet (blue) badlands, including four RCPs scenarios. Maps showing expected changes in moisture content of the soil layer for RCP2.6, RCP6.0 and RCP8.5 are shown in Supplementary Figure 7.

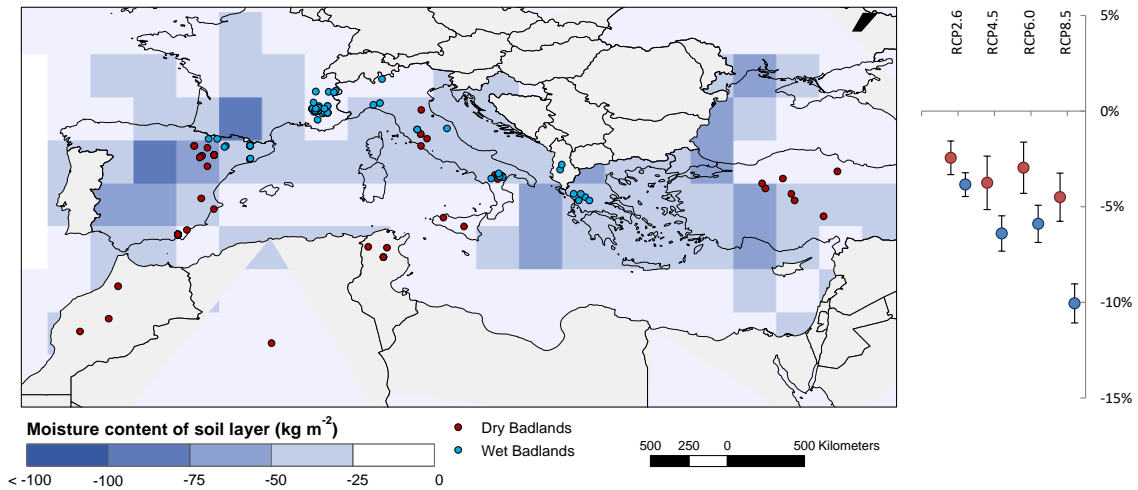


Table 1. Defining variables in badland areas in each operating process (weathering, hydrology and erosion) and climatic drivers considering in the analysis.

Defining variables			
Weathering	Hydrology	Erosion	Climatic drivers
Number of wetting-drying cycles Number of freezing cycles	Runoff coefficient Runoff rate Maximum peak flows	Sediment yield	Rainfall amount Rainfall intensity Timing/seasonality Wetting-drying cycles Freeze-thawing cycles Antecedent moisture

Supplementary Materials for

Mediterranean Badlands: their driving processes and climate change futures

Nadal-Romero, E.¹, Rodríguez-Caballero, E.^{2,3}, Chamizo, S.^{2,3}, Juez, C.¹, Cantón, Y.,^{2,3}
García-Ruiz, J.M.¹

¹ Instituto Pirenaico de Ecología, Consejo Superior de Investigaciones Científicas (IPE-CSIC), Campus de Aula Dei, P.O. Box 13.034, Zaragoza, Spain

² Department of Agronomy (Soil Science Area), University of Almería, Engineering High School, Almería, Spain

³ Centro de Investigación de Colecciones Científicas de la Universidad de Almería (CECOUAL), University of Almería, 04120 Almería, Spain

This PDF file includes:

Supplementary figures:

Supplementary Figure S1: A priori model showing the hypothesized causal relationships

Supplementary Figure S2: Sediment yield in dry and wet Mediterranean badlands

Supplementary Figure S3: Expected change in mean annual rainfall

Supplementary Figure S4: Expected change in mean simple daily intensity index

Supplementary Figure S5: Expected change in number of rainfall events

Supplementary figure S6: Expected change in number of frost days

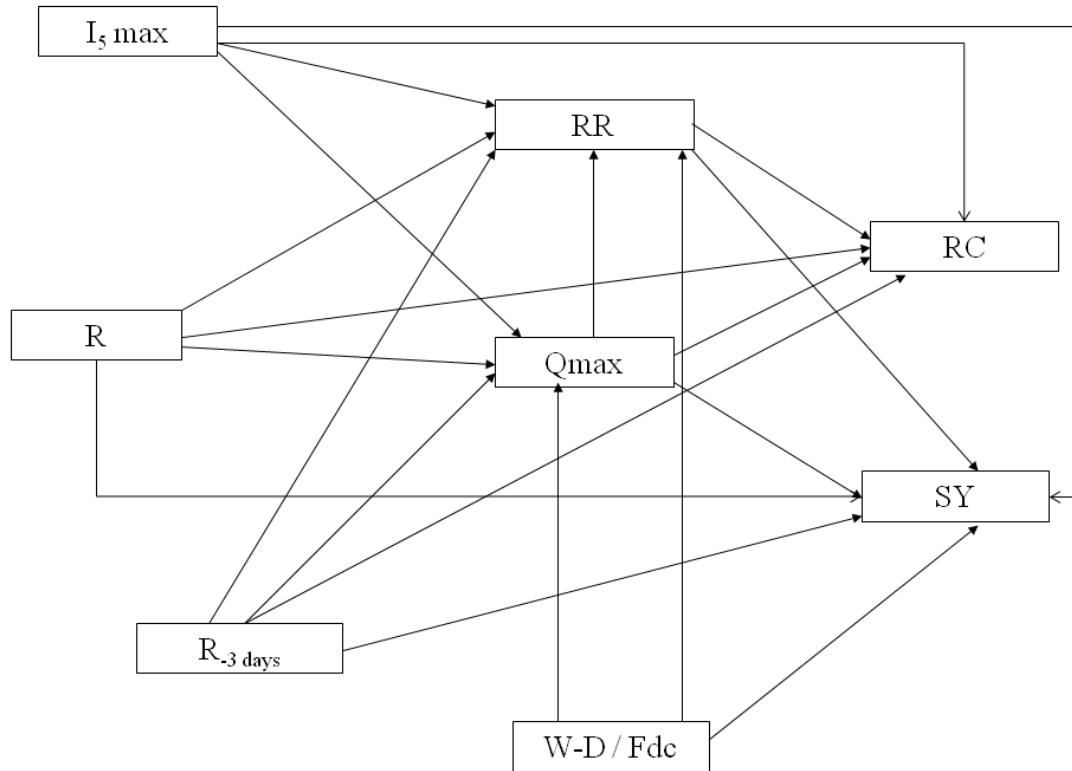
Supplementary Figure S7: Expected change in moisture content of the soil

Supplementary Figure S8: Expected change in extreme rainfall events

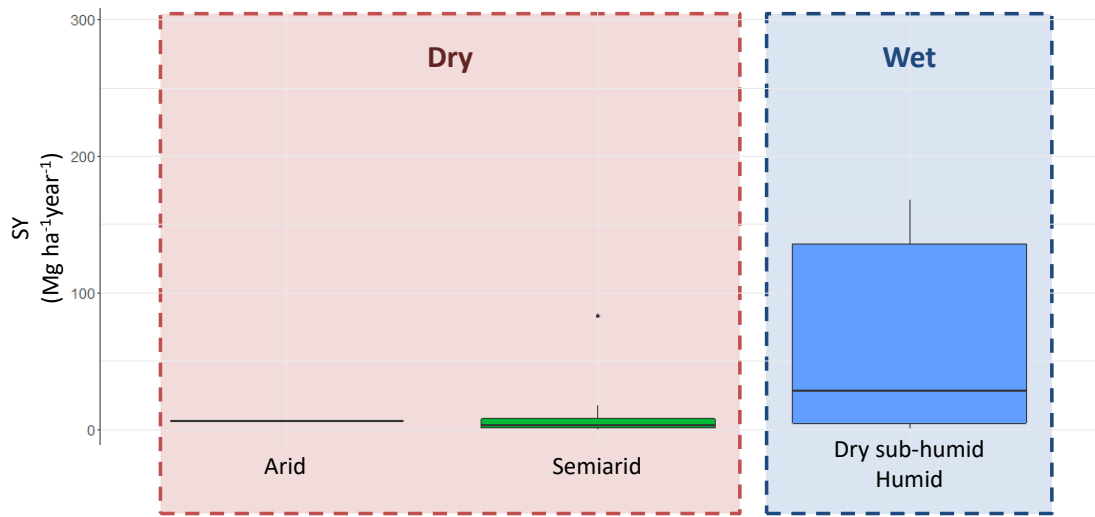
Supplementary tables:

Supplementary Table S1: Climate-drivers identified in Mediterranean badlands

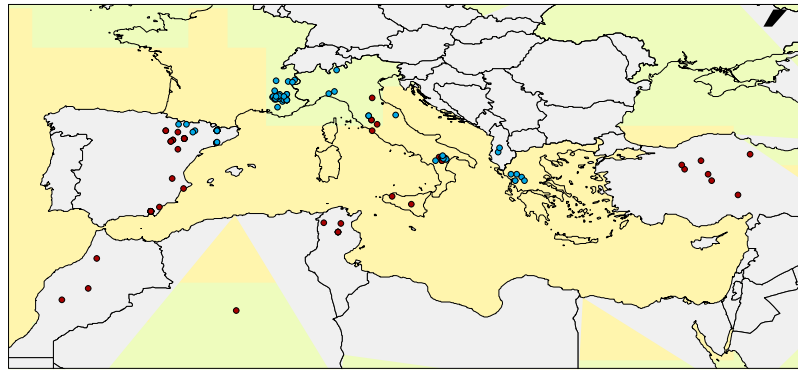
Supplementary Table S2: Results from SEM analyses



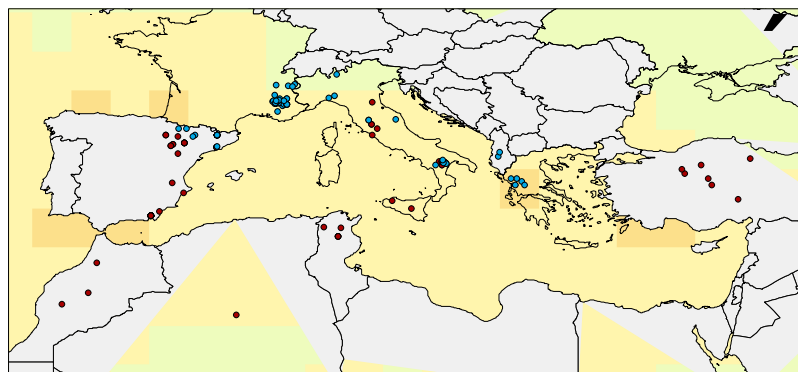
Supplementary Figure S1. A priori model showing the hypothesized causal relationships between the significant climate-drivers (Rainfall amount [R], maximum rainfall intensity in 5 min [$I_{5\max}$], 3-days antecedent rainfall [$R_{-3\text{ days}}$], and the weathering agent (number of wetting-drying [W-D] and freezing cycles 10 days previous to the event [Fdc for dry and wet badlands, respectively]) and the runoff (runoff rate [RR], runoff coefficient [RC] and Q_{\max}) and erosion response (sediment yield, SY).



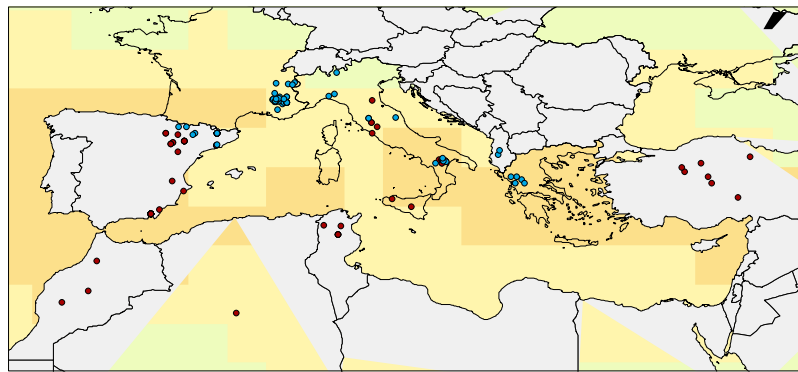
Supplementary Figure S2. Sediment yield (SY, Mg ha⁻¹ year⁻¹) in dry (arid and semiarid) and wet (subhumid and humid) Mediterranean badlands. Data from Nadal-Romero et al. (2011).



Mean anual precipitation change (mm / d year) ● Dry Badlands ● Wet Badlands 500 250 0 500 Kilometers

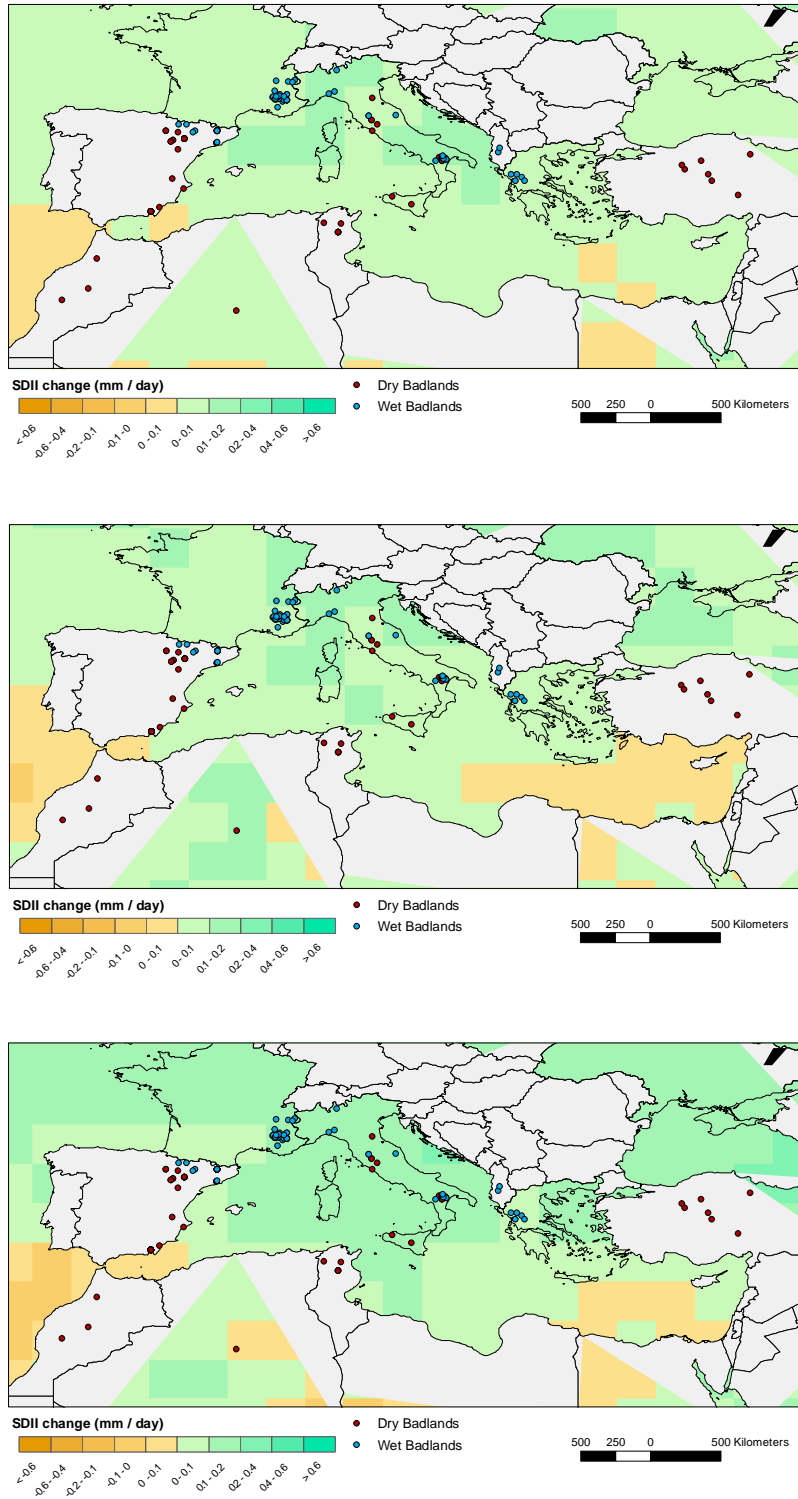


Mean anual precipitation change (mm / d year) ● Dry Badlands ● Wet Badlands 500 250 0 500 Kilometers

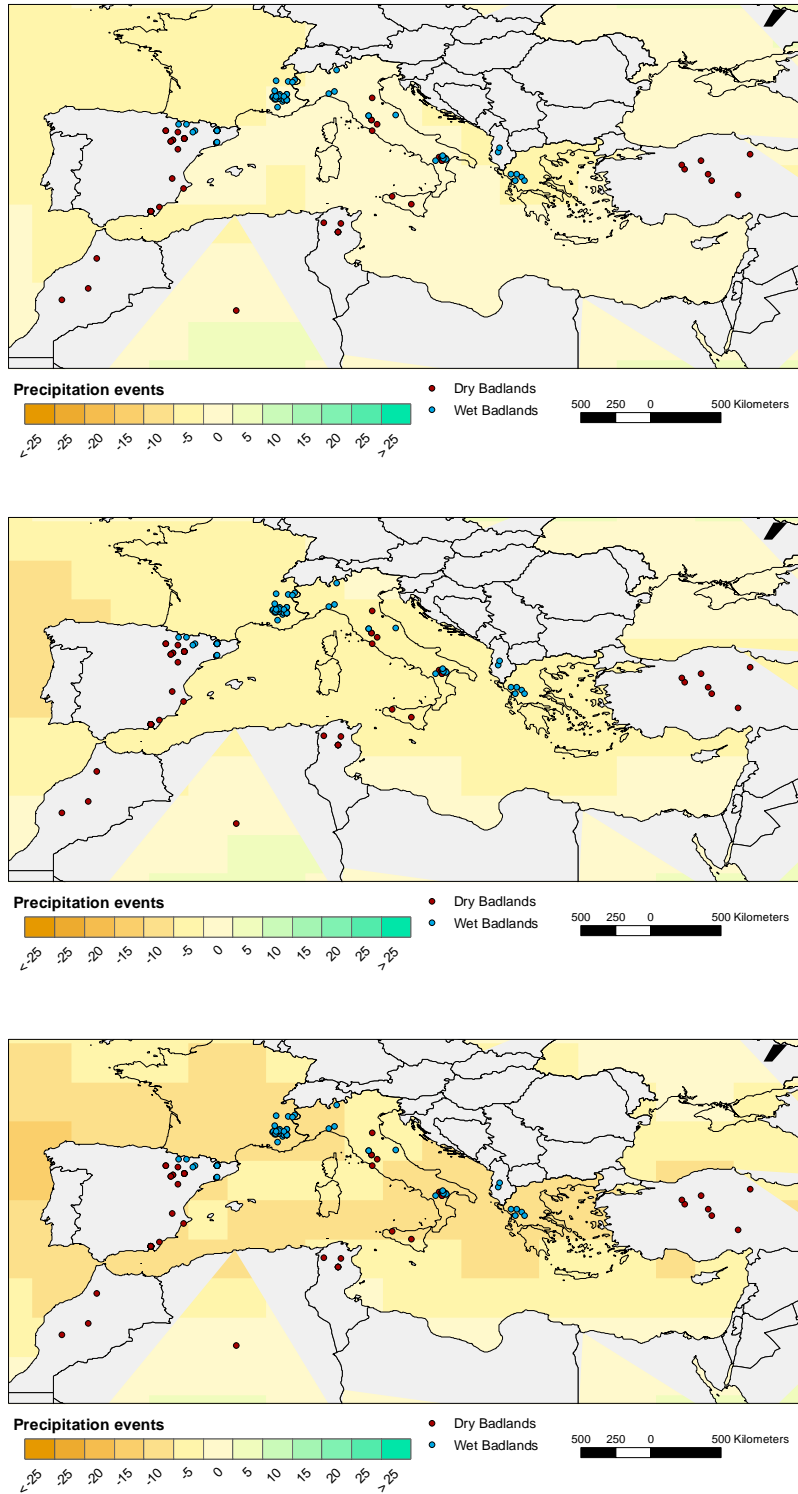


Mean anual precipitation change (mm / d year) ● Dry Badlands ● Wet Badlands 500 250 0 500 Kilometers

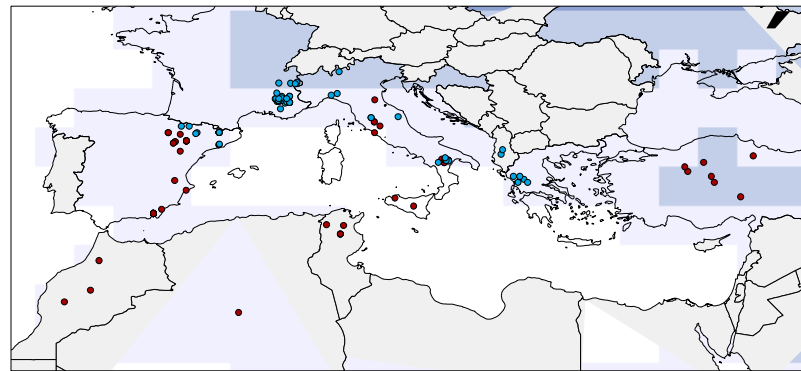
Supplementary Figure S3. Expected change in mean annual rainfall ($\text{mm d}^{-1} / \text{year}$) by the year 2050 compared to current conditions in the Mediterranean basin according to the a) RCP2.6 b) RCP6.0, and c) RCP8.5 of the fifth phase Climate Model Inter-Comparison P.



Supplementary Figure S4. Expected change in mean simple daily intensity index (SDII; Precipitation intensity index (mm/day) by the year 2050 compared to current conditions in the Mediterranean basin according to the a) RCP2.6 b) RCP6.0, and c) RCP8.5 of the fifth phase Climate Model Inter-Comparison Project.



Supplementary Figure S5. Expected change in the number of precipitation events (number of days with total rainfall > 1mm) by the year 2050 compared to current conditions in the Mediterranean basin according to the a) RCP2.6 b) RCP6.0, and c) RCP8.5 of the fifth phase Climate Model Inter-Comparison Project.

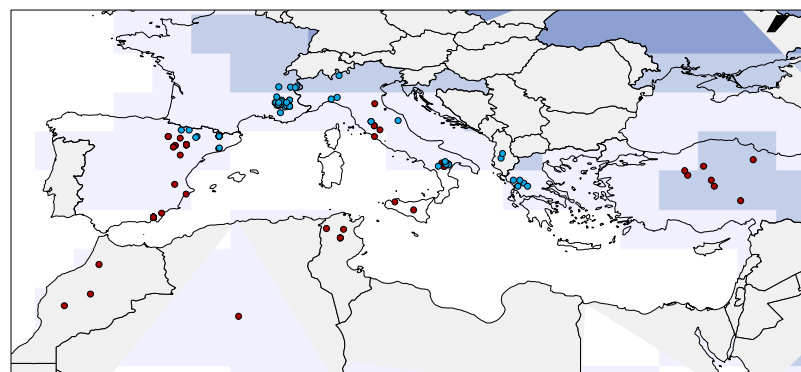


Number of frost days

● Dry Badlands
● Wet Badlands

500 250 0 500 Kilometers

-50 -40 -30 -20 -10 0

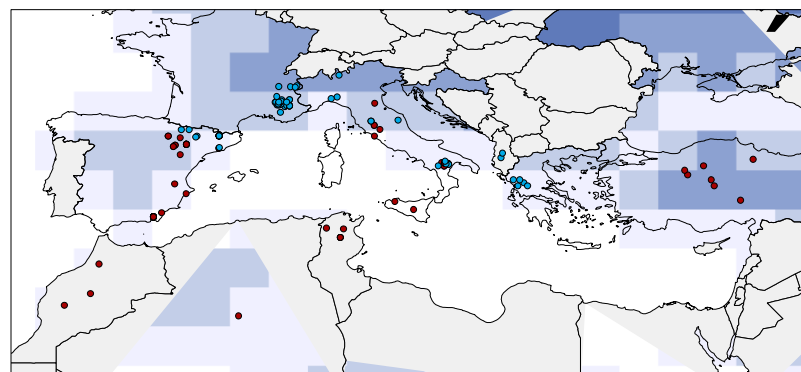


Number of frost days

● Dry Badlands
● Wet Badlands

500 250 0 500 Kilometers

-50 -40 -30 -20 -10 0



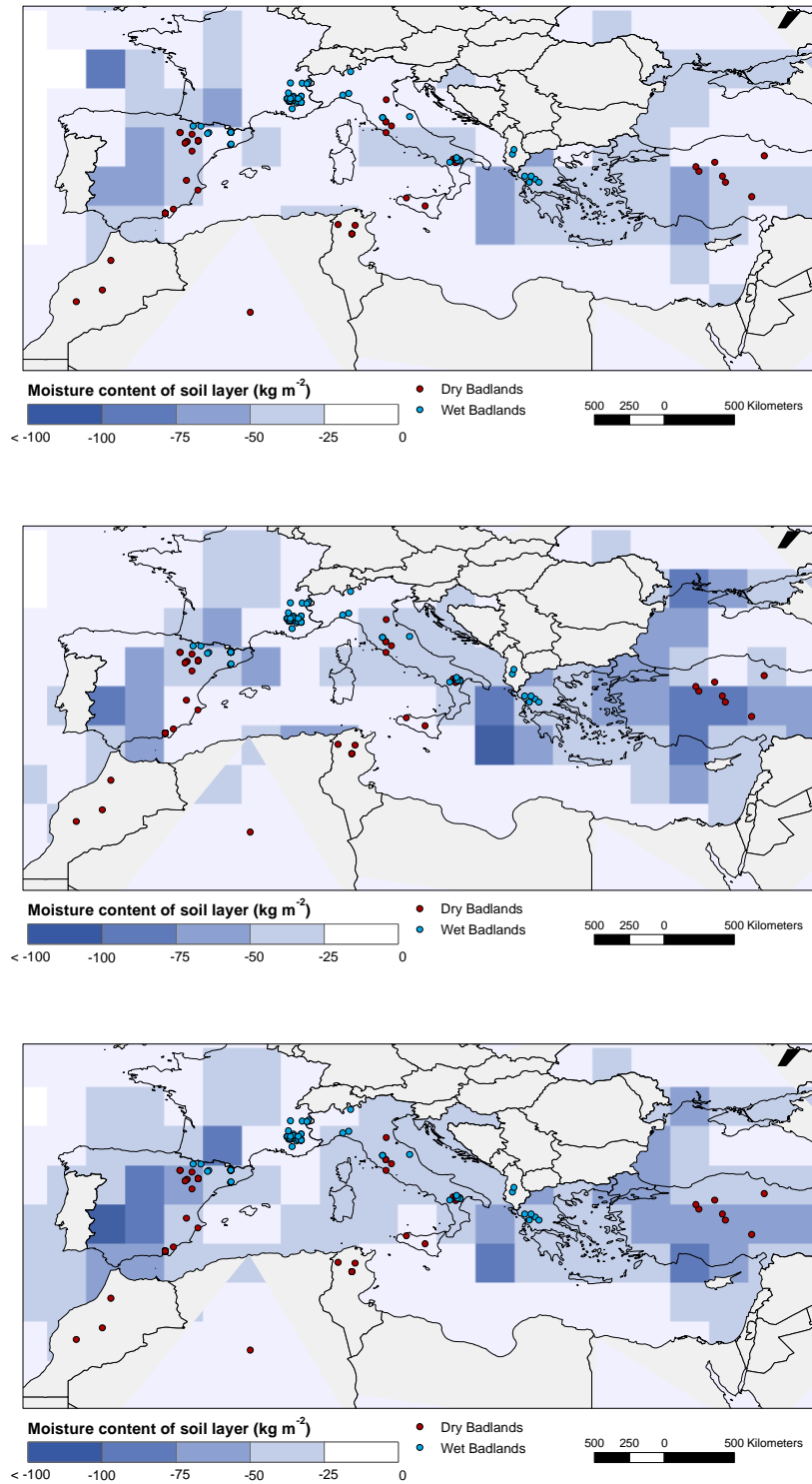
Number of frost days

● Dry Badlands
● Wet Badlands

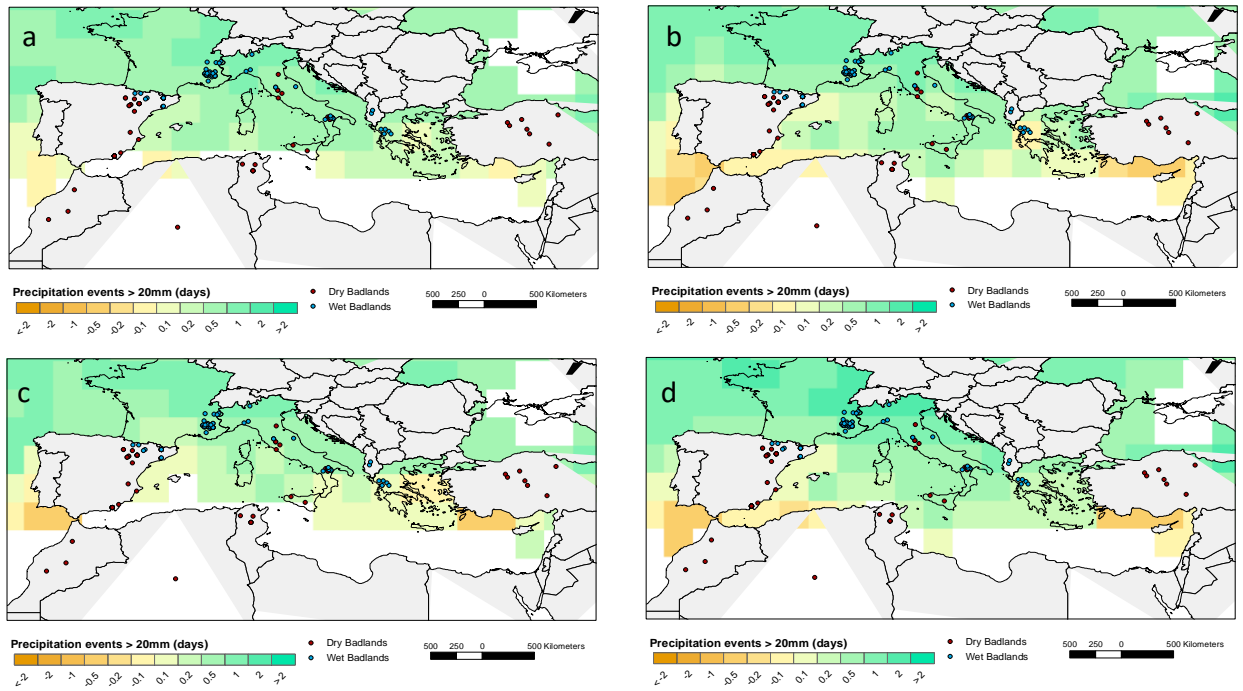
500 250 0 500 Kilometers

-50 -40 -30 -20 -10 0

Supplementary Figure S6. *Expected change in the number of frost days (number of days with mean temperature <math> < 0^\circ </math>) by the year 2050 compared to current conditions in the Mediterranean basin according to the a) RCP2.6 b) RCP6.0, and c) RCP8.5 of the fifth phase Climate Model Inter-Comparison Project.*



Supplementary Figure S7. *Expected change in moisture content of the soil layer (kg m⁻²) by the year 2050 compared to current conditions in the Mediterranean basin according to the a) RCP2.6 b) RCP6.0, and c) RCP8.5 of the fifth phase Climate Model Inter-Comparison Project.*



Supplementary Figure S8. *Expected change in extreme rainfall events (number of days with total rainfall > 20mm) by the year 2050 compared to current conditions in the Mediterranean basin according to the a) RCP2.6, b) RCP4.5, c) RCP6.0, and d) RCP8.5 of the fifth phase Climate Model Inter-Comparison Project.*

Supplementary Table S1. Main climate-drivers identified in the different study sites for weathering, hydrology and erosion processes.

Country, study site	MAP (mm)	MAT (°C)	Weathering drivers						Hydrology drivers						Erosion and Sediment yield drivers						References	
			R	W-D	F-T	Sn	T/S	Ant moist	R	I	W-D	F-T	T/S	Ant. moist	R	I	W-D	F-T	T/S	Ant. moist		
France, Pre Alps	900	10.9		•	•		•		•	•						•	•					2, 3, 14, 16, 28, 37
Israel, Zin Valley	91	17							•	•						•				•		21, 22, 44
Israel, West Bank	156-532	-							•	•												38
Italy, Basilicata	738	17														•	•	•		•		6, 10, 12, 13, 32, 33
Italy, Gran Gorgia	848	16				•										•	•	•				4
Italy, Northern Apennines	723	12.9														•	•					5
Italy, Upper Orcia	700	14														•	•			•		1, 6, 15,
Italy, Sicily	620	-															•			•		6
Italy, Calabria	700	19.7	•	•			•															34
Morocco, Eastern Rift	150-350	-																				42
Spain, Tabernas	235	17.8		•					•	•						•	•					8, 9, 39, 40, 41
Spain, Pyrenees	890	-																				11
Spain, Bardenas	350	13		•					•							•	•					17, 18
Spain, Eastern Pyrenees	862	9.1			•	•										•	•					19, 20, 29,
Spain, Isabena river	767	10			•				•							•						24, 25
Spain, Soto basin	755	13			•				•							•						23
Spain, Penedes	550	15		•												•	•					26, 27
Spain, Central Pyrenees	800	10			•				•								•					30, 31
Spain, Eastern Pyrenees	925	9			•			•	•							•		•	•			35, 36
Spain, Ebro	320	14							•								•					43
Tunisia, Souar	450	-														•						7
Relative importance (%) Dry badlands			14	72	0	0	14	0	56	33	0	0	0	11	30	35	15	0%	15	5		
Relative importance (%) Wet badlands			0	8	50	16	17	8	72	14	0	0	0	14	45	30	15	5	5	0		

MAP: Mean annual precipitation; MAT: mean annual temperature; W-D: wetting-drying cycles; F-T: freeze-thaw-cycles; Sn: snow; T/S: timing/seasonality; Ant moist: antecedent moisture; R: rainfall amount; I: rainfall intensity

References: [1] Aucelli *et al.* (2016); [2] Bechet *et al.* (2016); [3] Breton *et al.* (2016); [4] Bollati *et al.* (2019); [5] Bosino *et al.* (2019); [6] Brandolini *et al.* (2018); [7] Bouchnack *et al.* (2009); [8] Cantón *et al.* (2001a); [9] Cantón *et al.* (2003); [10] Capolongo *et al.*, (2008); [11] Castelltort (1995); [12] Clarke and Rendel (2006); [13] Clarke and Rendel (2010); [14] Crosaz and Dinger (1999); [15] Della Seta *et al.* (2009); [16] Descroix and Olivry (2002); [17] Desir and Marín (2007); [18] Desir and Marín (2013); [19] Gallart *et al.* (2013); [20] Guardià *et al.* (2000); [21] Khun and Yair (2004); [22] Khun *et al.* (2004); [23] Llena *et al.* (2020); [24] López-Tarazón *et al.* (2009); [25] López-Tarazón *et al.* (2010); [26] Martínez-Casasnovas *et al.* (2003); [27] Martínez-Casasnovas *et al.* (2004); [28] Mathys *et al.* (2003); [29] Moreno-de las Heras and Gallart (2016); [30] Nadal-Romero *et al.* (2010); [31] Nadal-Romero *et al.* (2018); [32] Piccarreta *et al.* 2006a; [33] Piccarreta *et al.* (2006b); [34] Pulice *et al.* (2013); [35] Regüés *et al.* (1995); [36] Regüés *et al.* (2000); [37] Rey (2009); [38] Ries *et al.* (2017); [39] Rodríguez-Caballero *et al.* (2014); [40] Rodríguez Caballero *et al.* (2015); [41] Rodríguez-Caballero *et al.* (2018); [42] Sadiki *et al.* (2017); [43] Sirvent *et al.* (1997); [44] Yair *et al.* (2013).

Supplementary Table S2. Direct, indirect and total effects among hydrological (i.e. **Supplementary Table S2.** Direct, indirect and total effects among hydrological (i.e. runoff rate [RR], runoff coefficient [RC] and maximum peak flows [Qmax] and sediment yield [SY]), and climate-drivers (rainfall amount [R], maximum rainfall intensity in 5 min [I₅max], 3-days antecedent rainfall [R_{-3 days}], and the number of wetting-drying [W-D] and freezing cycles 10 days previous the event [Fdc], for the two study cases, El Cautivo and Araguás catchments.

El Cautivo catchment	Direct effects				Indirect effects				Total effects			
	<i>RR</i>	<i>RC</i>	<i>Qmax</i>	<i>SY</i>	<i>RR</i>	<i>RC</i>	<i>Qmax</i>	<i>SY</i>	<i>RR</i>	<i>RC</i>	<i>Qmax</i>	<i>SY</i>
R	0.68	-0.49	0.33	0.27	0.13	0.85	0.00	0.27	0.33	0.37	0.81	0.54
R _{-3days}	0.00	0.08	0.02	0.17	0.01	0.01	0.00	0.01	0.02	0.09	0.00	0.17
I ₅ max	-0.11	0.10	0.46	0.04	0.17	0.07	0.00	0.22	0.46	0.17	0.06	0.27
RR	0.00	1.05	0.00	0.15	0.00	0.00	0.00	0.00	0.00	1.05	0.00	0.15
Qmax	0.38	0.02	0.00	0.47	0.00	0.40	0.00	0.06	0.38	0.41	0.00	0.52
W-D	-0.08	0.00	-0.02	-0.02	-0.01	-0.09	0.00	-0.02	-0.02	-0.09	-0.09	-0.04

Araguás catchment	Direct effects				Indirect effects				Total effects			
	<i>RR</i>	<i>RC</i>	<i>Qmax</i>	<i>SY</i>	<i>RR</i>	<i>RC</i>	<i>Qmax</i>	<i>SY</i>	<i>RR</i>	<i>RC</i>	<i>Qmax</i>	<i>SY</i>
R	0.67	-0.39	0.46	-0.22	0.17	0.78	0.00	0.51	0.84	0.40	0.46	0.29
R _{-3days}	0.16	0.12	0.22	-0.15	0.08	0.23	0.00	0.20	0.24	0.34	0.22	0.05
I ₅ max	-0.27	0.05	0.42	0.23	0.16	-0.09	0.00	0.20	-0.12	-0.03	0.42	0.43
RR	0.00	0.90	0.00	0.30	0.00	0.00	0.00	0.00	0.00	0.90	0.00	0.30
Qmax	0.37	0.05	0.00	0.56	0.00	0.33	0.00	0.11	0.37	0.39	0.00	0.68
Fdc	0.04	0.00	0.03	0.16	0.01	0.05	0.00	0.03	0.05	0.05	0.03	0.19